ADDIS ABABA UNIVERSITY

SCHOOL OF GRADUATE STUDIES

FACULTY OF SCIENCE

DEPARTMENT OF GEOLOGY AND GEOPHYSICS

THE GRAVITY FIELD, MAGNETIC FIELD AND REGIONAL TECTONIC SETTING OF THE CORBETTI CALDERA AND ITS ADJACENT AREAS.

BY

GETACHEW SHIFERAW

ADDIS ABABA

JUNE, 1999

THE GRAVITY FIELD, MAGNETIC FIELD AND REGIONAL TECTONIC SETTING OF THE CORBETTI CALDERA AND ITS ADJACENT AREAS

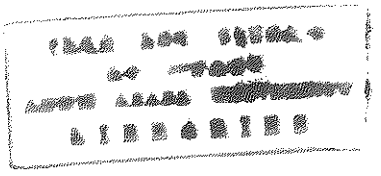

A Thesis submitted to the School of Graduate Studies of Addis Ababa University in partial fulfillment for the Degree of Master of Science in Geophysics

BY

GETACHEW SHIFERAW

JUNE, 1999

ABSTRACT

In this thesis work analysis of about 2220 gravity and 75 magnetic data collected in the Lakes District of the Main Ethiopia Rift (MER), between latitudes 6.88° - 7.75° and longitudes 38.00° - 39.00° consisting of the Corbetti caldera is made.

A gravity survey covering about an area of 12100 sq. kms with observation points of about 2220 stations are discussed (about 50 gravity and 75 magnetic stations, were occupied during field work by the author of this thesis and Dr. Abera Alemu, advisor to this thesis work, while the rest of gravity data were obtained from the Ethiopian Institute of Geological Surveys and the Geophysical Observatory of Addis Ababa University). Both the magnetic and gravity data sets are of semi-regional type, with station separations ranging on the average from about 1-10 km.

The analysis includes compilation in a standard format of the recent and the previous gravity data sets, which required homogenisation to IGSN-71 datum from the previous surveys that was found out not available in this datum.

The theoretical (normal) gravity values for each stations were calculated by means of the international gravity formula (GRS-67) and all gravity field stations are tied to the IGNS-71 datum of the Geophysical Observatory of Addis Ababa University (whose gravity value is

977452.16 mGal). Similarly, the magnetic data are also drift corrected for the diurnal variations.

Results of both the gravity and magnetic surveys have revealed significant achievements in mapping several zones of hydrothermal alterations, weak structural indications such as faults, lineaments, fractures, joints, etc. within the study area. The delineation of weak structural features and hydrothermal manifestations i.e. altered grounds with fumarolic activities that are associated with fissures, craters, faults and caldera rims, where tectonic structures give major access for hydrothermal fluids which in turn are favourable for economic mineral potentials like sulphides, epitermal gold deposits, etc. In addition, to these invaluable natural resources these data are also important in the mapping and location of potential geothermal zones. Both the gravity anomaly maps and the magnetic anomalies are found in agreement in mapping of the geological and structural trends. The distinction between the rift and the adjacent plateaus and the regional structure features were depicted from the anomaly maps on the basis of the general shape and wavelengths of the anomalies.

ACKNOWLEDGMENTS

First and foremost I should offer my thanks to God without whose strong support this work would have been impossible. I am very grateful to the Aquatic Private Ltd. Company for the sponsorship of the field work expenses.

I express my deepest gratitude to my principal advisor Dr. Abera Alemu for his advice, concern, encouragement and proper guidance through out the progress of this thesis work. Moreover, I am greatly indebted to him for providing me with the necessary materials and for making arrangements to consult him any time and use materials of his own that is of great importance to this thesis work. I also wish to thank my co-advisor Dr. Solomon Tadesse, Head of the Department of Geology and Geophysics for his advises and for making arrangements to have access to the computer facility of the Department.

I have to express my sincere appreciation to my co-advisors Ato Ayele Teklu and Ato Girma Wolde Tinsae for their advises, proper help and assistance. I am also grateful to Ato Berhanu Bekele, head Geophysics Department of Ethiopian Institute of Geological Surveys (E.I.G.S) and Ato Befekadu Oluma, head Regional and Air-borne Geophysics Team (E.I.G.S), Ato Bekana Muleta, head Mineral Exploration Team (E.I.G.S), Ato Kimemu Nure, Ato Binyam Wondirad (who was kindly assisting all the 1999 graduating geophysics students in computer mapping), Ato Mamushet Zewge, Ato Senay Mekuria and also other mambers of the Geophysics Department (E.I.G.S) whose names are not listed here are greatly acknowledged.

TABLE OF CONTENTS

	page
Abstract	i
Acknowledgments	iii
Table of contents	iv
List of figures	vii
CHAPTER 1. INTRODUCTION	1
1.1 Location	1
1.2 Object and overview of the Thesis	1
CHAPTER 2. GEOLOGICAL AND TECTONIC REVIEW	4
2.1 Geologic and tectonic setting of the Ethiopian Rift system	4
2.2 Geology and tectonic setting of the Main Ethiopian Rift	6
2.3 Geology of Corbetti area	7
CHAPTER 3. PREVIOUS GEOPHYSICAL STUDIES AND RESULTS	10
3.1 The resistivity survey	10

page

3.2 The gravity survey 11

3.3 Conclusion and recommendation 11

CHAPTER 4. THE THEORY OF GRAVITY AND MAGNETIC METHODS 13

Introduction 13

4.1 The earth's potential methods in general 13

4.2 The gravity method 15

4.2.1 Fundamental Principles of gravity 15

4.2.2 Basic theory of gravity 18

4.2.3 The normal (theoretical) gravity equation 21

4.2.4 The reduction of gravity data 25

4.2.5 Gravity anomaly maps 31

4.3 The magnetic method 34

4.3.1 Fundamental principles of magnetism 34

4.3.2 Magnetism of the earth 37

4.3.3 Magnetism of rocks and minerals 42

page

CHAPTER 5. THE GRAVITY AND MAGNETIC DATA 44

5.1 Introduction 44

5.2 Data preparation and processing 45

5.3 Assessment of errors in the gravity anomalies 49

5.4 Compilation of the gravity anomaly maps 59

5.5 Interpretation of gravity data 60

5.5.1 Bouguer anomaly map 60

5.5.2 The free air anomaly map 62

5.5.3 The residual anomaly map 63

5.5.4 The regional anomaly map 64

5.6 Interpretation of magnetic data 64

CHAPTER 6. CONCLUSIONS AND RECOMMENDATIONS 66

6.1 Discussion 66

6.2 Conclusions and Recommendations 67

REFERENCES 70

CHAPTER 1

INTRODUCTION

1.1 LOCATION

The Study area is located in the central part of the Main Ethiopia Rift (MER), between latitudes 6.88°N-7.75°N and longitudes 38.00°E- 39.00°E (Fig. 1) that encompasses an area of about 12100 sq kms and within which the Corbetti caldera is consisted.

The Corbetti caldera is bounded by lake Awasa to the south and lake Shalla to the north (Fig. 1), with geographic location between latitudes 7.17°N-7.25°N and longitudes 38.30°E and 38.47°E.

1.2. OBJECT AND OVERVIEW OF THE STUDY

This M.Sc. research is devoted to the analysis and interpretation of about 2220 gravity and about 75 magnetic data collected in the study area cited. The gravity data coverage incorporates the area limited by the location of the study area; while the magnetic data is confined to the area limited by the location of the Corbetti caldera cited above.

As the survey is semi-reconnaissance type, accessibility to all the stations was possible using four wheel drive (with the exception to very few limited traverses that were occupied on foot). These data will be analysed to test the applicability of the methods in the study region and identification of subsurface geological bodies and structures with the following objectives:

-to compile the previous data obtained from the involved agencies like EIGS, A.A.U. and the data acquired under this survey with datum homogenisation, reduction and compilation in a standard format of all the available gravity data acquired within the survey area so far, i.e. a homogenisation to the same datum (IGSN-71 Datum) and reference system (GRS -1967).

- to produce anomaly maps appropriate to each method , of the study area with the homogenised version of the compiled data set.

- to make a preliminary qualitative interpretation from the resulting anomaly maps appropriate to each method in terms of the geologic and tectonic features of the study region, and compare the results obtained with the previous works aforementioned, i.e. interpretation of the gravity and magnetic anomaly patterns (distribution, location, and orientation of the anomalies) resulting from the compiled anomaly maps in terms of variations in density and susceptibility of near surface and sub-surface geological bodies and structural features residing beneath the study area.

- to compare the results (gravity anomalies and anomaly maps) of the homogenised data set with that of its earlier version (i.e., obtained from the agencies mentioned and found out to be heterogeneous).

- to generate the magnetic anomaly map of the area over which magnetic observations are made and compare the resulting magnetic anomalies with those of the corresponding gravity anomalies.

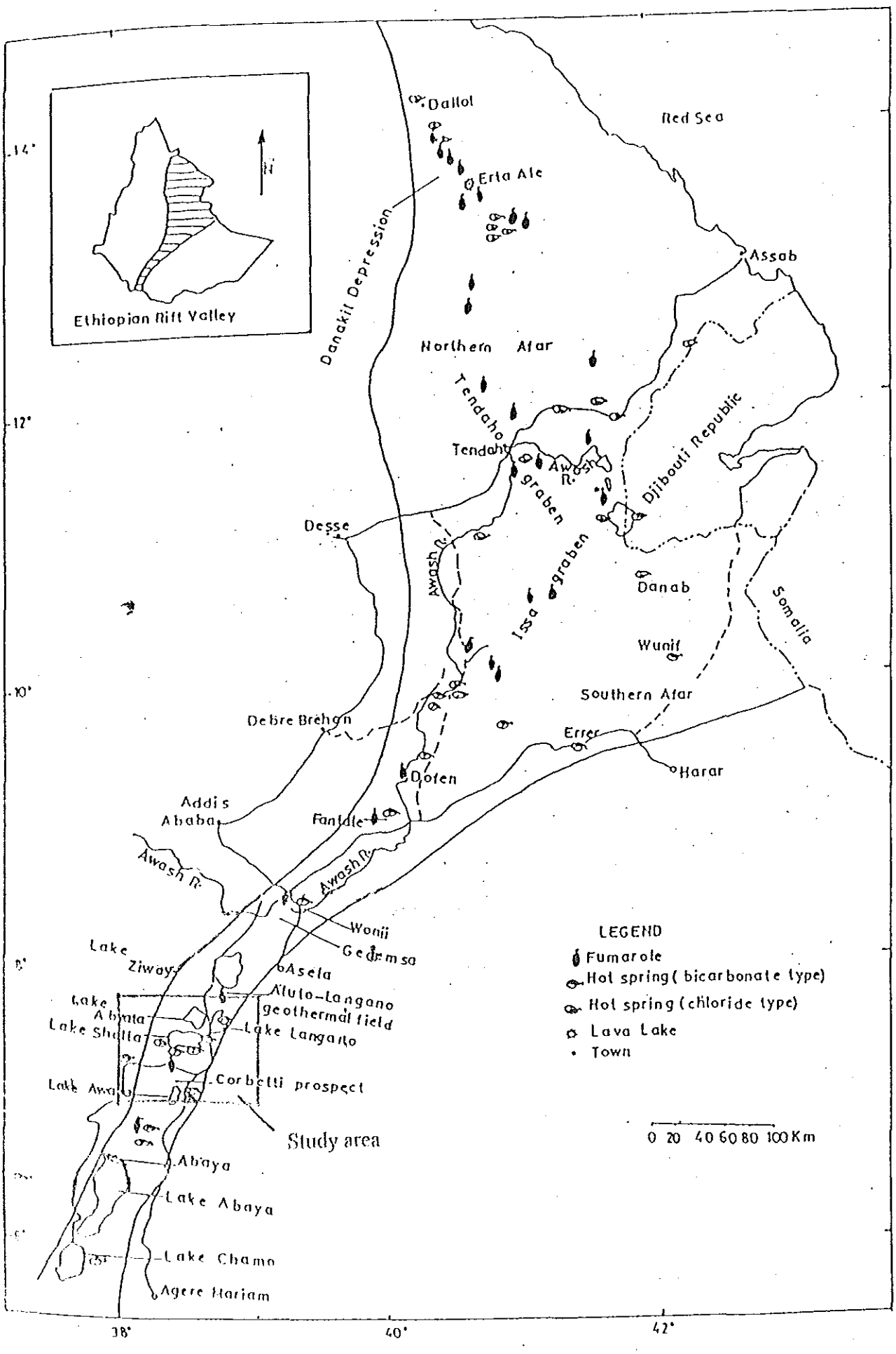

Fig. (1) Location map of the study area (Corbetti and its surroundings)

- to determine the type of geologic bodies generating the gravity and magnetic anomalies based upon the similarities and differences the two anomalies exhibit or reveal.

The generated anomaly maps give a first hand reliable information in the distribution, location and orientation of the geological structures of the area that is inconsistent with the field observations and the geological map of the area. Moreover, the compiled data is believed to contribute a bit to the national challenge in the compilation of a homogenised gravity data catalogue of the country.

The thesis is organised in six chapters. The first chapter is introduction to the thesis. The second and third chapters discuss the previous geological and geophysical works in the study area. The fourth chapter addresses the theoretical basis of gravity and magnetic methods. In the fifth chapter, a discussion on the field work, data reduction, assessment of the associated errors, compilation of the observed anomaly maps and a qualitative description and interpretation of the anomalies in terms of the major geologic and tectonic structures of the rift system and the neighbouring regions in comparison with results obtained from earlier geological and geophysical surveys as a constraint etc. is presented. The last chapter deals with conclusions and recommendations.

CHAPTER 2

GEOLOGICAL AND TECTONIC REVIEW

2.1. GEOLOGIC AND TECTONIC SETTING OF THE ETHIOPIAN RIFT SYSTEM

The term Ethiopian Rift System is used to designate the three descrete rift segments, namely the Afar depression, the Main Ethiopian Rift (MER) and the Southern Ethiopian Rifts (SER). This rift system is part of the Great East African Rift System, widely believed to have been formed by diverging lithospheric plates, active since early Tertiary times. The Great East African Rift itself is part of the Afro-Arabian Rift System that extends for about 6500 km from Turkey to Mozambique (Mohr, 1962)

The great mass of pre-rift volcanic rocks in Ethiopia is perceived by Almond (1986) as directly related to the initial phase of rapid extension across the Red Sea and Gulf of Aden axes at a time when the Afar triple junction was first being formed. He concluded that before early Miocene there was no recognisable Afro-Arabian dome.

The wide-spread late Eocene uplift in the Ethio-Arabian region, indicated by rapid marine regression, which is considered to be the formation of the Eastern Rift system uplift and axial down-wrapping. In Ethiopia these phases were preceded and accompanied by outpouring of the Eocene-Oligocene trap series fissure basalts. Uplift of the Ethiopian dome has been synchronous with the major pulses of late Mid-Miocene and Plio-Pleistocene age. Volcanism of intermediate

andesitic type shows some relation to uplift in time and space and to the on set of graben faulting, but major flood basalt extrusions in the early Tertiary in Ethiopia were related to massive crustal warping along the future rift margins (Baker et al. 1972). Mohr (1971) proposed three episodes of swell uplift in Ethiopia; the late Eocene, middle Miocene and late Pliocene-early Pleistocene.

Di Paola and Berehe (1979) noted the occurrence of a Precambrian basement (150 m thick) at Kela horst, with a cover of typical Mesozoic marine sediments as a result of pre-Trappean tectonic movement, within the MER and close to the western margin. Having recognised greater thickness of the lithosphere along the western margin of the rift relative to the eastern margin from the nature of the Quaternary basalts of Butajira-Silti and Bishoftu ranges and from magmatological differences they signify along the eastern margin of the Ethiopian rift.

The mid Tertiary rise of the Ethiopian dome (Mohr 1962, Baker, et al 1972) was accompanied by further down wraping along the margins of at least 1000 m magnitude. This post-Pliocene rift, which associated with major graben faulting in the MER, took place in the lower and middle Pleistocene, and notably affect drainage patterns on the rift shoulders.

The process of rifting was always preceded by a long period of uplift; in the case of younger rifts the uplift is related to the rise of hot, low density material from the mantle and formation of a transitional layer at the base of the crust. Development of rifts joined in a triple junction was not simultaneous but arose from differential rift movements initiated at different times - the Gulf of Aden in the early Miocene, the Red Sea in the late Cretaceous, the Afar in the lower Miocene or Oligocene, and the MER in the Pliocene or late Miocene. There were periods when rifting

occurred in one of the rifts while the adjoining rift remained passive, example; during the early Mesozoic and late Cretaceous-Pliocene (Kazmin, 1979).

In the upper Pliocene, voluminous fissure and central eruptions of trachyte-pantelleritic ignimbrites covered most of the southern Ethiopian plateau and filled the MER. The source situated chiefly at the rift margins, which ranges in thickness from about 300 m to 500 m. The thickness in the rift floor are probably greater (Mohr 1968, Baker et al. 1972).

The inner graben on the rift floor is cut by numerous small vertical faults and open fissures. Flows in the late Quaternary minor amounts of flood basalts have emerged from some of these faults. The inner graben is also the location of dormant silicic caldera volcanoes whose eruption product commonly fill the graben.

2.2 GEOLOGIC AND TECTONIC SETTING OF THE MAIN ETHIOPIAN RIFT

Initiation of the MER was in late Tertiary times. By the Pliocene there was a shallow trough with a deep infilling of silicic volcanics, dominated by ignimbrites originating from a center close to the rift margins. A major episode of uplift and graben faulting early in the pleistocene created the lofty escarpments of the rift margins. Subsequent tectonic fragmentation of the rift floor formed the Wonji fault belt, a narrow NNE trending fault zone disposed en-echelon along the floor, and uncommon to transverse faults such as those east of the Aluto volcano and Corbetti caldera.

Concomitant volcanism broke out on the rift floor giving rise to volcanic centers such as Aluto, Shalla and Corbetti. The main products are lavas and pyroclastics ranging from trachytes to pantelleritic rhyolites in composition (Lloyd, 1977, Kazmin, 1980).The rift floor in the Lakes District rift basin is occupied by Pliocene-Quaternary sediments and volcanics, all but the youngest of which are cut by the Wonji fault belt. The rift is marked by a set of NNE-SSW normal faults. "En-echelon" arrangements, rift in rift structures, asymmetry and open tensional fissures are its most important tectonic features with associated volcanic activity, both fissural and through central vents.

2.3 GEOLOGY OF CORBETTI AREA

Post caldera activity around Corbetti area is represented with the birth of three recent peralkaline volcanoes (Urji, Chebbi and Danshe). The Corbetti caldera is elliptical in shape; the minor axis is about 10 km N-S and the major axis is about 18 km E-W.

As to the geological compositions, it is within a recent volcano tectonic activities on Wonji fault belt, mainly composed of per alkali-silicic products, rhyolite flows, obsidians, pumice, ashes, ignimbrites and the same nature of basaltic lava flows and scoria. There are pre and post caldera sediments and recent alluvium. All volcanic formations indicate starting from early formation of the caldera to the plio-pleistocene activities which are characteristic of the MER (Elias Altaye 1983).

The caldera comprises fissure eruptions, which were followed by a volcano-tectonic collapse. The volcanoes are all at a fumarolic stage. Urji and Danshe volcanoes are formed of pyroclastics which are represented by pumice flows and pumice falls; on the eastern side of Urji some obsidians enterbedded with pumice outcrop. Chebbi volcano is mostly formed of pumice like Urji. The difference between the three volcanoes is the amount of very recent obsidian lava flows which cover the pyroclastics of Chebbi (Dipaola 1972).

Chabbei volcano is extruded from the eastern segment of the caldera ring fractures, but east west tectonics may also be an important factor controlling its location. The east west alignment evident on Urji are even more evident on Chebbi because the pyroclastic over burden is less or absent. Present east-west sub-parallel fissure swarms cut the lava flows independent of their flow direction and are probably the surface expression of deep tectonic weakness evidenced also by a major east-west fault, down thrown south, which appears east of Chebbi and gains topographic expression east words (UNDP Tech. Report 1973).

There are many occurrences of fumaroles (steam vents) and hot ground (hot springs) in several places within the caldera. In general most of the hydrothermal manifestations are associated with recent volcanological fractures such as eruption centers, craters and caldera rims, controlled by structural features (faults, fissures, joints, and contact zones). Hydrothermal manifestations i.e., altered grounds with fumarolic activities are associated with fissures, craters, faults and caldera rims, where tectonic structures give major access for hydrothermal fluids.

These zones of fumeroles and structural features are supposed to be favorable zones for potential mineral deposit like epitermal gold, sulfides, etc. and also geothermal resource areas which usually are zones of alterations.

CHAPTER 3

PREVIOUS GEOPHYSICAL STUDIES AND RESULTS

Extensive geological and geophysical surveys had been carried out by the Ethiopian Institute of Geological surveys (E.I.G.S), under a project called Geothermal Exploration Project in the search for geothermal resource. The geophysical surveys carried out consists of electrical resistivity mainly vertical electrical sounding (VES), gravity and also self potential (SP) methods.

3.1 THE RESISTIVITY SURVEY

The resistivity survey (VES) was carried out using a Schlumberger array for large depths of investigation i.e. AB/2 upto 3160 m (unpublished report of the project 1983) and also dipole dipole method with a spacing a = 500 m (distance between the centers of potential and current electrodes) were used.

Results of the survey shows that a low resistivity zone extending from the Corbetti caldera north ward to southern shore of lake Shalla bounded by a 20 ohm-m contour and decreasing inwards. The low resistivity zone is associated with a channel of hot geothermal water flow from the caldera north wards to lake Shalla and hence a heat source is inferred to exist under the Caldera. The flow is chiefly along a channel causing hot springs on the southern shores of lakes Chitu and Shalla, controlled by geologic structures and topography.

3.2 THE GRAVITY SURVEY

The main features indicated by the Bouguer gravity map are: a large two dimensional gravity high is oriented in a NW-SE direction which includes the Corbetti caldera. This anomalous zone is characterized by intensive surface fumarolic activity. A small relative positive anomaly is opening to Wondo Genet which has hot springs located at the eastern margin of the rift. A large relative negative anomaly is located west of lake Awasa. East of lake Awasa another relative negative anomaly is opening to the south, to the Awasa basin. The residual gravity map indicates three major localities of positive anomalies. It is associated with fumarolic activities beginning from the Corbetti caldera and extending NW wards.

3.3 CONCLUSION AND RECOMMENDATION

From both the resistivity and gravity surveys and additional geological mapping (by Elias Altaye) the following conclusions had been arrived at:

- Thermal manifestations are controlled by fault systems and fissures running east west to which Artu-Dima and Urji thermal manifestations are related to volcanic cones, craters, centers of recent volcanic activities such as Chabbi, Urji and Danshe volcanoes and NNE trending fault system

- Chabi volcano seems to have a better economic geothermal potential inspite of the difficult

access for detailed exploration

- Interpretation of the available data had revealed Corbetti caldera is a heat source for the thermal manifestations and lake Shalla is a sink where hot geothermal fluid mixes with ground water and is being supplied to it controlled by geological structure related to the NNE trending Wonji fault belt, indicated by the low resistivity strip extending from Corbetti caldera to lake Shalla where it broadens around the southern shore of the lake. These broadening are due to the movement of the thermal fluid towards the lake sediments in addition to the clay content in the sediments.

- The recommendations suggested were

(a) to continue the resistivity work for better delineation and refinement of the anomalous resistivity zones in the Corbetti caldera,

(b) to understand the inter-relation of the thermal manifestations and the mechanism of heat transfer few drilling wells had been recommended at some selected localities.

CHAPTER 4

THEORY OF GRAVITY AND MAGNETIC METHODS

INTRODUCTION

The basic theories of gravity and magnetic methods are compiled from lecture notes of the post graduate course entitled "Gravity and Magnetic Methods - Geo 564" delivered by Dr. Abera Alemu and standard text books in geophysics (such as written by Dobrin, Parasnis, Telford, etc.).

4.1.THE EARTH'S POTENTIAL METHODS IN GENERAL

The gravity and magnetic survey methods exploit the fact that variations in the physical properties of rocks in-situ give rise to variations in some physical quantity which may be measured remotely - at the ground surface or above it- without the need to touch, see, or disturb the rock itself.

The value of the methods is that these observed variations when corrected appropriately for predictable or measurable non-geologic effects and presented as 2-D maps of "anomalies" over the earth's surface-may be interpreted in terms of 3-D subsurface variations of rock properties. These physical property variations must relate, to a greater or lesser extent, to what we loosely term the "geology" of the subsurface (Paterson, J.R. And C.V. Reeves, 1985).

Both gravity and magnetic methods, therefore, employ a two stage process: (1) measurement of anomalies at or above the ground surface; and (2) interpretation of anomalies in terms of rock property variations within the subsurface in a way which adds to knowledge of the geology.

In the case of the gravity methods, the physical property of rocks is density, and density variations at all depths within the earth contribute to the broad spectrum of the gravity anomalies. Density, in turn, depends upon the porosity and gross mineralogy of rocks in bulk.

In contrast, for the magnetic method, the rock property is magnetic susceptibility and / or remnant magnetisation, both of which can only exist at temperatures cooler than the Curie point, restricting the source of magnetic anomalies to the upper most 30-40km of the earth's interior. In practice, almost all magnetic properties of rocks in bulk reflect the properties and concentrations of a single accessory mineral magnetite, which signals a caution in relating magnetic surveys to geology.

Progress in interpretation and geologic synthesis has been continual in the case of gravity method; however, only recently (Emerson, 1979; Grant 1985 a, b) has any serious effort been made to determine the relationship between magnetite distribution and geologic processes. Geologic models are essential at all stages in application of the two methods. In the survey design phase (and methodology) it is important to know the probable size, depth, and geometry of the targets of interest. In the interpretation phase it is only through the use of geological constraints that we can overcome the inherent problem of non uniqueness of potential field interpretation.

Stated simply, the geophysicist is concerned not only finding a physical property distribution that best fits the observed data, but also with distribution that is consistent with what is already known about the geology and what is geologically reasonable to speculate about the unknown. It is within this limits that new geologic information may be obtained from potential field data.

Since both methods are limited to investigation of geologic structures which are represented by density and / or magnetic content contrasts, these practical applications may appear quite limited. However, compared with alternative methods of discovering anything about the subsurface (of which drilling is perhaps is the most obvious example), they have the advantages of being orders of magnitude less expensive. In fact, no other methods can tell us so much for so little cost. The continuing demand for gravity and magnetic data around the world is ample evidence of this (Telford, 1980).

4.2 THE GRAVITY METHOD

4.2.1 Fundamental Principles of Gravity

The expression of gravitational attraction in a form most useful for application to exploration requires an understanding of the basic physical connects relating force, acceleration and potential.

Gravitational force: is based on Newton's law expressing the force of mutual attraction between two particles in terms of their masses and separation. This law states that two very small

particles of mass m_1 and m_2, respectively, each with dimensions very small compared with the separation r of their centers of mass, will be attracted to one another with a force

$$\mathbf{F} = -G\,(m_1 m_2/r^2)\mathbf{e}_r \qquad (4.1)$$

where G, known as the universal gravitational constant & its value $6.67*10^{-11}$ $m^3/kg\ s^2$

F is the force on m_2,

$\mathbf{e}_r$ is a unit vector directed from m_1 to m_2.

The negative sign indicates that the force is always attractive. The expression of gravitational attraction in a form most useful to exploration requires an understanding of the basic physical concepts relating force, acceleration & potential.

Gravitational acceleration: considering the earth's mass (M), the gravitational attraction of a spherical, non-rotating, homogeneous earth of mass M and radius R on a small mass m on its surface acts as though its mass is concentrated at the center of the sphere. Therefore,

$$\mathbf{F} = (GMm/r^2)\mathbf{e}_r = m\mathbf{g} \qquad (4.2)$$

Force is related to mass by acceleration; the term

$$\mathbf{g} = (GM/r^2)\mathbf{e}_r \qquad (4.3)$$

is called the gravitational attraction or intensity of gravitational attraction or simply gravity (**g**).

The gravitational acceleration at the earth's surface is taken about 980 cm/sec^2 or 980 Gal (named after Gallileo, who conducted pioneering research on the earth's gravity).

Gravity units: in exploration work we are likely to be measuring differences in acceleration one ten-millionth or less of the earth's field. Fundamentally, the SI unit for acceleration / gravity is m/sec^2. The sub-unit, one m/sec^2 is called one gravity unit (g.u.).For convenience in working with gravity data obtained for geological & geodetic studies the milliGal (mgal, 1/1000 Gal) has come to be the common unit for expressing gravitational accelerations. For conversion,

$$1 \text{ cm/s}^2 = 1 \text{ Gal}$$

$$1 \text{ m/s}^2 = 10^5 \text{ mGal}$$

$$1 \text{ m/s}^2 = 1 \text{ gu}$$

Gravitational Potential: As the intensity of gravitational, magnetic, or electric fields depends only on position, the analysis of such fields can often be simplified by using the concept of potential. The potential at a point in a unit mass from an arbitrary reference point (usually at an infinite distance) to the point in question. The intensity of gravitational field is defined in terms of gravitational potential as:

$$U = Gm/r \qquad (4.4)$$

where U is a scalar quantity, m is the mass being attracted by another unit mass and r is the separation between the two masses. The first derivative of U in any direction gives the component of gravity in that direction, as a result a potential field approach provides computational flexibility. Equipotential surfaces are regions where U is constant. The sea-level

surface, or geoid, is the most easily recognized equipotential surface, which is assumed to be horizontal and orthogonal to the direction of gravity.

4.2.2 Basic theory of gravity

Consider a small mass (m) moving with a velocity **V** on the surface of the earth that is rotating with

angular velocity ω, (Fig. 4.1)

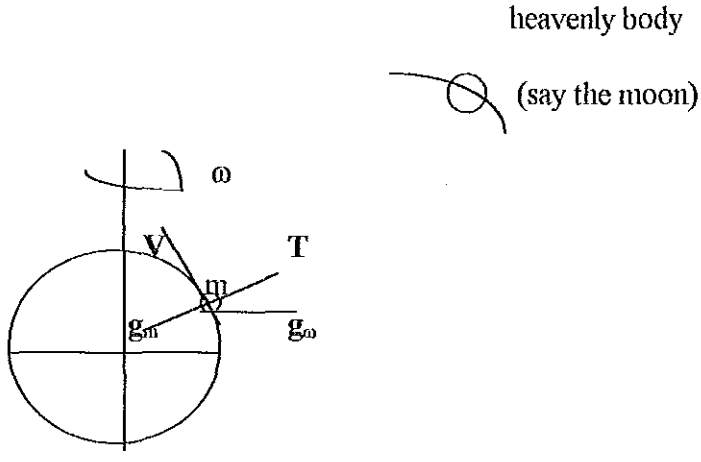

Fig. 4.1 Forces acting on a mass located on the surface of the rotating spherical earth model

The resultant force per unit mass acting on mass m is,

$$\mathbf{g} = \mathbf{g}_m + \mathbf{g}_\omega + \mathbf{c} + \mathbf{T} \qquad (4.5)$$

which is known as gravity, where $\mathbf{g}_m$ is attractive force per unit mass acting on m due to earth's mass, $\mathbf{g}_\omega$ is centrifugal force per unit mass acting on m due to earth's rotation, with angular velocity ω, **c** is the coriolis force per unit mass acting on m due to its motion, **T** is tidal force per

unit mass acting on m due to mass attraction of other heavenly bodies.

The effect of the forces **c** & **T** on the gravity **g** is usually considered negligible in local work. Thus, **g** refers to the combined effects of both earth's mass gravitation $\mathbf{g}_m$ and rotation $\mathbf{g}_\omega$, which are given by the relations,

$$\mathbf{g}_m = (GM/R^2)\mathbf{e}_r \qquad (4.6)$$

$$\mathbf{g}_\omega = (\omega \times R) \qquad (4.7)$$

$$\mathbf{g} = \mathbf{g}_m + \mathbf{g}_\omega$$

$$= (GM/R^2)\mathbf{e}_r + \omega(\omega \times R) \qquad (4.8)$$

Since the force $\mathbf{g}_\omega$ has both the tangential and radial components, the radial component which is $\omega^2 R \cos^2\phi$ is opposite in direction with the attractive force, thus

$$g = (GM/R^2) - \omega^2 R \cos^2\phi \qquad (4.9)$$

which is the basic equation of gravitational acceleration or intensity of gravitational acceleration. If we let the intensity of gravity at the equator g_e where $\phi = 0°$ and that at poles g_p where $\phi = \pm 90°$,then

$$g_e = GM/R^2 - \omega^2 R \qquad (4.10)$$

and

$$g_p = GM/R^2 \qquad (4.11)$$

If we compute the intensity of gravity for a spherical symmetric earth model, one obtains the gravity difference as,

$$g_p - g_e \approx 3.4 \text{ Gal} \qquad (4.12)$$

But, form the actual observations of the real earth, the measured values are;

$$g_p = 983.218 \text{ cm/s}^2 \text{ (or Gal)}$$

$$g_e = 978.072 \text{ cm/s}^2$$

and

$$g_p - g_e \approx 5.2 \text{ cm/s}^2 \qquad (4.13)$$

The discrepancy or disagreement between the observed and calculated values of g indicate various aspects, of which some are:

- the shape of the earth is not spherical,
- the shape of the earth is a rotationally distorted one such that its shape is flattened at the poles and bulged at the equator,

- g varies as a function of latitude (ϕ).

4.2.3 The Normal (theoretical) Gravity equation

Due to the centrifugal force, the earth's shape departs form a sphere, i.e., it is bulged at the equator and flattened at the poles. That is, the effect of the centrifugal force gives the earth the shape of more or less an ellipsoid of revolution, i.e., a surface generated by the rotation of an ellipse about its minor axis with the major axis generating the equatorial plane.

To determine the gravity field of the earth at a point we must know its shape & density distribution. For describing the earth's shape, one usually uses as a reference an ellipsoid of revolution with Z-axis coinciding with the axis of the earth's rotation and XY plane with the equatorial plane. We assume that the ideal reference ellipsoid, which is related to the mean sea level surface with excess land masses removed and ocean deeps filled, is an equipotential surface of a normal gravity field. Denoting the potential of the normal gravity field by $U = U(x,y,z)$, we see that the reference ellipsoid is a surface with,

$$U(x,y,z) = Uo = \text{constant} \qquad (4.14)$$

The earth's gravity potential, U, is the sum of the attractive potential (V) and the centrifugal potential (Φ) given by,

$$U = V + \Phi = G \int_v dm/r + 1/2\ \omega^2(x^2 + y^2) \qquad (4.15)$$

The normal gravity vector γ_ϕ at a given latitude ϕ on the reference ellipsoid is the gradient of U.

$$\gamma_\phi = \text{grad}\ (U) \qquad (4.16)$$

After few mathematical computations, one can arrive at the normal gravity field or theoretical gravity value, γ_ϕ as a function of the latitude angle ϕ , at any pint on this ellipsoid is given by

$$\gamma_\phi = \gamma_o(1 + B_1 \sin^2\phi - B_2 \sin^2 2\phi) \qquad (4.17)$$

where γ_o is the value of gravity at the equator $\phi = 0$, B_1 & B_2 have been determined in 1930 by the International Association of Geodesy (IAG) and adopted the formula known as the 1930 International Gravity Formula given as,

$$\gamma_{\phi 1930} = 978049\ (1 + 0.0052884\ SIN^2\phi - 0.0000059\ SIN^2 2\phi)\ \text{mGal} \qquad (4.18)$$

with γ_o = 978049 mGal, equatorial radius a = 6378.388 Km, polar radius b = 6356.909 Km, the ellipticity (polar flattening) given by,

$$f = (a - b)/\ b = 1/127 \qquad (4.19)$$

Recent studies on the orbits of satellites have provided precise values for the determination of the constants B_1 & B_2 and the following is the revised theoretical gravity formula established by IAG in 1967.

$$\gamma_{\phi 1967} = 978031.85(1 + 0.0053024 \sin^2\phi - 0.0000059 \sin^2 2\phi) \text{ mGal} \qquad (4.20)$$

with γ_o = 978031.85 mGal, a = 6378.160 Km, b = 6356.909 Km and f = 1/129.25 Even in its most refined state, the standard theoretical gravity formula is a very crude approximation. It assumes that there are no undulations on the earth's surface, where as, in fact w have on the real earth's surface elevated lands (such as mountains, hills, etc.) and depressions (such as valleys, oceanic depressions, etc).

Hence, for a practical work, i.e., measurement of gravity on the physical surface of the earth we must define a physical equipotential surface on the earth. The physical surface is known as the Geoid. Geoid is a surface such that gravity g is perpendicular to it. It is a zero reference (elevation datum h = 0) for elevations and ocean depths, as given on topographic maps. Geoid is the undisturbed mean sea level surface continued into continents so as to encircle the earth, water seeking its level in imaginary shallow canals until it is at rest. The value of gravity at a point calculated by a standard theoretical formula and that observed and reduced to the geoid do not agree with each other. This is because the effect of attraction of an invisible anomalous mass under the point is involved in the observed value. The small difference between the actual gravity potential W(x,y,z) and the normal (theoretical) gravity potential U(x,y,z) is denoted by T(x,y,z)

shown below in (Fig.4.2), so that

$$W(x,y,z) = U(x,y,z) + T(x,y,z) \qquad (4.21)$$

T is called the anomalous potential, or disturbing potential (Heiskanen and Moritz, 1967). For small regions T is negligible. Thus we compare the potential on the geoid referred to mean sea level surface given by

$$W(x,y,z) = W_o \qquad (4.22)$$

with the potential on the reference ellipsoid referred to the same mean sea level surface given by

$$U(X,Y,Z) = U_o \qquad (4.23)$$

on the assumption that they are potentials of the same equipotential surfaces i.e.,

$$U_o = W_o \qquad (4.24)$$

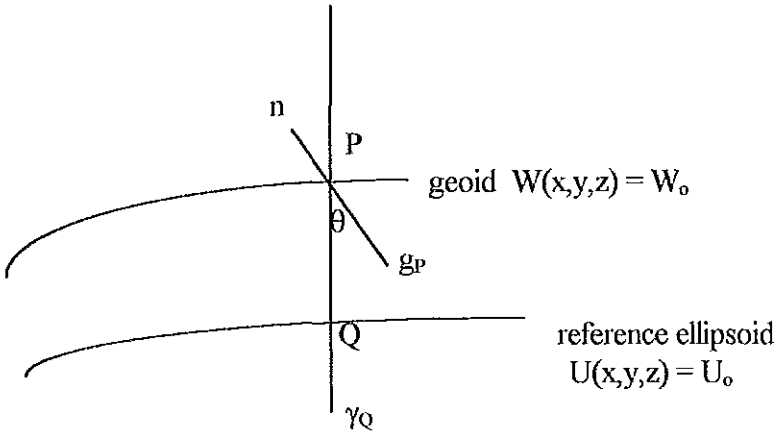

Fig. 4.2 Geoid and reference ellipsoid

Consider now the gravity vector g_p at a point P of the geoid (Fig. 4.2) and the normal gravity vector γ_Q at point Q of the ellipsoid. The gravity anomaly vector Δg is defined as their difference in magnitude given as,

$$\Delta g = g_P - \gamma_Q \qquad (4.25)$$

The difference in direction is the deflection of the vertical (θ). Hence g_p is the gravity value observed ($g_{obs.}$) at a point on the surface of the earth and reduced to the geoid point (p). γ_Q is the theoretical gravity value on the ellipsoid point (Q).

Gravity anomalies are developed as a consequence of differences in density distribution of the earth, particularly in the upper layers known as the crust. Therefore, they reflect the internal constitution of the crust & indicate the presence of various geological structures connected with the dislocation of rocks of different densities. This enables us to study and give clues about geological constituents, structural features such as faults, lineaments, fissures, etc. of the earth and for gravity prospecting technique.

4.2.4 The reduction of gravity data

In reality, the earth's gravity (g) is measured at points on its surface. On the other hand, since the earth's surface does not represent a regularized equilibrium surface g varies because of variations

in latitude, elevation, topography of the surrounding terrain, earth tides and subsurface density variations. g is not directly comparable with the normal sea level gravity (γ) referring to the surface of the ellipsoid. Hence, a reduction of g to an equipotential sea level surface (geoid) is necessary. These reductions must attempt to produce the value of g that would have occurred if it were possible to observe on the geoid surface. The manner in which g is reduced to the geoid to compute the different gravity anomalies is known as gravity reduction. All the stations occupied in the study area have been referred to the International Gravity Standardization Net - 1971 (called IGSN -1971) (Morellei et al. 1971) gravity datum. The primary gravity base of the Geophysical Observatory (with gravity value of 977452.16 mGal) of Addis Ababa University which is referred to the IGSN-71 datum by the U.S. Defence Mapping Authority Aerospace Center in 1973 was used. The theoretical gravity, γ, at latitude ϕ, has been calculated from the 1967 gravity formula (Geodetic reference system 1967, Moritz, 1971) given by Eq.(4.20) is with an accuracy of $\pm$ 0.4 mGal. As gravity measurements are not made on the ellipsoid but usually on earth's surface at some height h above a reference equipotential surface (mean sea level or geoid), reductions must be applied to the observed values before any anomaly may be obtained. Different types of anomalies are possible depending upon the manner in which this correction is computed.

In general the corrections brought to an accurate gravimetric survey are of many natures, but they can be classified under corrections for,

(a) Instrumental correction (drift or time variation of gravimeters)

In practice, all gravimeters have a certain amount of drift. This time variation may be due to many causes (example: slight temperature and / or pressure variation even if the instrument is self-compensated) but more commonly due to the fact that the quartz springs are not perfectly elastic and are subject to creep over a certain period of time. The drift in the gravimeter reading at a station may be from a few hundredths of a mGal to four tenths of a mGal per hour. In order to correct for drift, one or more stations were reoccupied at intervals of one to three hours. Assuming the drift of the gravimeter is linear, the differences between two readings at a station were plotted against time. Corrections were read off & applied to the intermediate stations readings.

(b) Tidal correction (earth tide correction)

The combined attraction of the sun & the moon may change the gravity at a station cyclically with a maximum daily amplitude of 0.3 mGal. Appropriate corrections can be made by referring to special tables. (example, tables regularly published in advance for each year in Geophysical Prospecting, the Journal of the European Association of Exploration Geophysicists). Since tidal variations are rather slow, it is assumed that their effects will fully be incorporated in the instrumental drift correction. In the present work tidal effects were assumed to be included in the drift correction according to the manual of the gravimeter.

(c) Elevation (free-air) reduction

The elevation reduction to the geoid, through the height h, neglecting the matter contained between the geoid and the earth's surface (free-air correction) is obtained by the inverse square law, and this variation of gravity with height is expressed by:

$$\delta g_f = -(\partial g/\partial h)h \approx -(\partial \gamma/\partial h)h \approx 0.3086h \text{ mGal} \qquad (4.26)$$

where h is height above sea level in meters. This constant factor (0.3086 mGal/m) has been used throughout the computation of the free-air correction.

(d) Bouguer correction

The attraction of the material between the reference equipotential surface (ellipsoidal or geoidal surface) and that of the individual gravity station is taken care by the Bouguer correction. If a given station is higher than the reference ellipsoid or geoid or sea-level, its gravity value is increased because of the attraction of the slab of material between it and the reference level and the correction is negative. If the station is lower than the reference elevation, its gravity value is decreased because of the lack of attraction of the absent material between it and the reference geoidal level and the correction is positive. Therefore the Bouguer correction is always opposite in sign to the free air correction.

In order to account for the effect of masses between the geoid and the observation point, the

gravitational attraction of an infinite horizontal slab of rock material of thickness equal to the station height h and density (normally 2.67 gm/cm^3) was computed using the known slab). The Bouguer correction is given by

$$\delta g_b = 2\pi g\rho h = 0.0419\rho h = 0.1119 \text{ mGal} \qquad (4.27)$$

(e) Terrain correction

A topographic irregularity (hill, valley, slope, etc.) will exert an attraction directly proportional to its density. The vertical component of this attraction will be directed upwards and reduce the gravity at the point of measurement. This magnitude must therefore be added to the measured value of gravity at the point. A valley is a negative mass and the vertical component of its attraction will also be directed upwards leading again to an additive topographic correction. There are several methods for calculating terrain correction. Hammer (1939) illustrated the necessity of making terrain corrections. If precise gravity surveys are desired terrain correction tables with which this quantity may be determined to the accuracy merited by the precision of modern gravimeters.

The usual procedure is to divide the area around a station in compartments bounded by concentric rings and their radii drawn at a suitable angular interval. The mean elevation (Z) in each compartment is determined from a topographic map, without regard to sign, i.e., by treating a hill as well as a valley as positive height difference form the station level. The calculation of the

tables is based upon the formula for the gravitational attraction of a vertical hollow cylinder at a point .on the axis and in the plane of one end of the cylinder; and the equation for terrain correction is,

$$\delta g_t = 2\pi G\rho h(r_2 - r_1 + (r_1^2 + Z^2)^{1/2} - (r_2 + Z)^{1/2}) \qquad (4.28)$$

where r_1, r_2 are the inner and outer radii respectively, and Z is the height of the cylinder (representing the average height of the terrain or elevation)

Note that, the terrain correction δg_t attains 0.1 - 1.0 mGal in flat areas and 10 - 100 mGal in mountainous areas.

Gravimetric surveys in hilly country like the study area are subject to errors which may be much larger than the probable errors of the unreduced gravity values unless accurate correction are made for the non-significant gravitational effects of the undulating topography.

(h) Latitude correction

If the earth were a homogeneous non rotating sphere with the same vertical gradient everywhere, apart from local near surface, density variations due to geological structures, and if it were a perfectly smooth surface, then clearly all gravity variations over the surface would be caused by geological structure. But this is not so. Because of the flattening, the poles are nearer to the center of mass than the equator, sot the gravity increases with increasing in latitude. The

variation of gravity with latitude over the surface of an ellipsoid earth can be expressed by the revised theoretical gravity formula established by IAG in 1967 (Eq. 4.20)

The latitude correction $\delta\gamma_\phi$ is obtained by differentiating Eq (4.20) with respect to ϕ and is added to g as we move towards the equator, i.e.,

$$\delta\gamma_\phi/\delta s = (-1/R)\delta\gamma_\phi/\delta_\phi = 0.811 \sin 2\phi \text{ mGal/km} \qquad (4.29)$$

where R is the radius of the earth (= 6371 km), s = R = N-S horizontal distance, and is latitude angle.

4.2.5 Gravity anomaly maps

The end result of a gravity survey is to produce gravity anomaly maps such as the Free-air, the Simple Bouguer Anomaly (S.B.A), the Complete Bouguer Anomaly (C.B.A), etc. maps these maps re geophysical tools upon which effects of geology on the earth's gravity field can be detected and determined. These effects are indicated by patterns (contours & curves) of gravity anomaly variations over the survey area.

After all of the preceding gravity corrections were applied to the observed gravity reading of each station, the gravity anomalies thus obtained are:

(a) The Free-air anomaly

- It generally forms the basis for the interpretation of gravity data, mainly in marine environment, but however, it can also serve for land gravity surveys.

- The free air anomaly is given by the equation

$$\Delta g_f = g_{obs} \pm \delta g_f - \gamma_\phi \qquad (4.30)$$

where Δg_f is the free-air anomaly, gobs is the observed gravity value of the station $\pm \delta g_f$ is the free-air correction which is 0.3086 h (h is elevation in m) the + sign is if the survey is carried on the surface above the reference geoidal surface, and the - sign is if the survey is carried below the reference geoidal surface, γ_ϕ is the normal / theoretical gravity value computed for the stations latitude value using the 1967 gravity formula, which is Eq. (4.20)

(b) The Simple Bouguer Anomaly (S.B.A)

- The simple Bouguer anomaly is a gravity anomaly that accounts for the Bouguer slab (which is given by $0.0419\rho h$, where ρ is density of the surrounding materials in g/cm^3 and h is elevation in m), and the free-air correction.

Note that the simple Bouguer anomaly doesn't account for the terrain correction (δg_t).

- The simple Bouguer anomaly is given by the Eq.

$$\Delta g_{SBA} = g_{obs} \pm \delta g_f + \delta g_B - \gamma_o \qquad (4.31)$$

For the case of the study area, which is above the geoidal surface this equation becomes

$$\Delta g_{SBA} = g_{obs} + (0.3086 - 0.0419\rho)h - \gamma_\phi \qquad (4.32)$$

(c) The Complete Bouguer Anomaly (C.B.A) or simply the Bouguer Anomaly

- This anomaly takes into account the free-air correction, the Bouguer slab and the terrain correction.

- It is given by the equation

$$\Delta g_{CBA} = \Delta g_B = g_{obs} \pm \delta g_f - \delta g_B + \delta g_t - \gamma_\phi \qquad (4.33)$$

For the case of the study area, the Eq reduces to

$$\Delta g_B = g_{obs} + (0.3086 - 0.0419\rho)h + \delta g_t - \gamma_\phi \qquad (4.34)$$

Note: Apart from the above discussed major anomaly maps there are also other maps such as the residual gravity anomaly map, the regional gravity anomaly map, etc.

4.3 MAGNETIC METHOD

4.3.1 Fundamental principles of magnetism

(a) Magnetic force: If two poles of strength p_o and p ,respectively, are separated by a distance r, the force F between them will be

$$F = p_o p/\mu r^2 \qquad (4.35)$$

The constant μ, known as the permeability, depends upon the magnetic properties of the medium in which the poles are situated. The units of pole strength are determined by the specification that F is 1 dyne when two unit poles 1 cm apart are situated in a nonmagnetic medium such as air or vacuum (for which $\mu = 1$).

Note that the similarity between the magnetic force and the gravitational force, the latter expressing gravitational attraction between two particles. If the poles are like type, the force is repulsive, if they are unlike it is attractive.

(b) Magnetic field: The magnetic field strength at a point is defined as the force per unit of pole strength which would be exerted upon a small pole of strength P_o if placed at that point. Thus, the field strength H due to a pole strength P a distance r away is

$$H = F/p_o = p/\mu r^2 \qquad (4.36)$$

The magnetic field strength is often expressed in terms of the density of the lines of force or flux representing the field. The unit of H is then expressed as one line of force per square cm. It may also be designated in the cgs system as one dyne per unit pole or as one Oersted. In the MKS system, the unit of flux density is the Tesla, which is 10^4 Oe.

In magnetic prospecting we measure variations of the order of $1/10^4$ of the earth's magnetic field, which is about 0.5 Oersted. A new unit of magnetic intensity or field strength, the gamma (γ), is introduced

$$1\,\gamma = 10^{-5} \text{ Oerested}$$

This unit is a convenient size for geophysical work. Still additional smaller unit is the nanoTesla.

$$1\,\gamma = 1 \text{ nanoTesla (nT)}$$

(c) Magnetic moment: The magnetic poles always exist in pairs, the fundamental magnetic entity is the magnetic dipole, two poles of strength +m and -m separated by a distance l. Then the magnetic moment is defined as

$$M = mlr_1 = \mu r_1 \qquad (4.37)$$

M being a vector in the direction of the unit vector r_1 extending from the negative pole towards the positive pole.

(d) Intensity of magnetization: A magnetic body placed in an external magnetic field becomes magnetized by induction. The intensity of magnetization is proportional to the strength of the field and its direction is in the direction of that field. It is defined as the magnetic moment per unit volume, that is,

$$I = M/V = ir_1 \qquad (4.38)$$

Practically this magnetization by induction amounts to lining up the dipoles of the magnetic material; for this reason I is often referred to as the magnetic polarization. If I is constant and has the same direction throughout, the body is said to be uniformly magnetized.

(e) Magnetic Susceptibility: The degree to which the body is magnetized is determine by its magnetic susceptibility, defined as

$$K = I/H \quad \text{or} \quad I = KH \qquad (4.39)$$

Susceptibility is the fundamental parameter in magnetic prospecting, since the magnetic response of rocks and minerals is determined by the amount of magnetic materials in them and the latter have K values much larger than the rocks and minerals themselves.

(f) Magnetic induction: The magnetic body which we are considering, when placed in the external

field H, has its internal poles more or less lined up by the field H to produce a field of its own H', which increased the total field within the body. This extra field is related to the intensity of magnetization. The magnetic induction ,B, is defined as the total field within the body and can be written

$$B = H + H' = H + 4\pi I$$

$$B = (1 + 4\pi K)\, H \qquad (4.40)$$

Now by definition the ratio of induction B to magnetizing force H is the magnetic permeability, μ, thus,

$$B = \mu H \qquad (4.41)$$

4.3.2 Magnetism of the earth

It is well established that the geomagnetic field is composed of three parts, so for as exploration geophysics is concerned: the main field, the external field and variations of the main field.

(i) The main field, which although not constant in time, varies relatively slowly and is of internal origin.

(a) Elements of the earth's magnetic field

If a steel needle, not previously magnetized, could be hung at its center by a thread so that it were free to orient itself in any direction in space, at most points on the earth's surface it would assume a direction neither horizontal nor in line with the geographical meridian. This orientation is the direction of the earth's total magnetic field at this point. The magnitude of this field, F, the inclination of the needle from the horizontal, I, and its declination, D, the angle it makes with geographic north, completely define the magnetic field. The various magnetic elements are illustrated in Fig.(4.3) below .

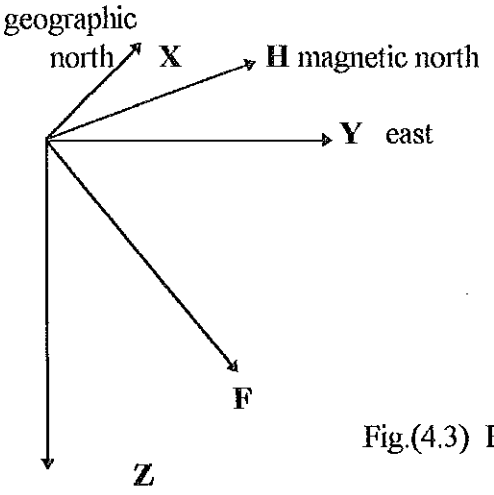

Fig.(4.3) Elements of the earth's magnetic field

In addition to F,I and D, there are the vertical component Z, the horizontal component H which in turn have components X and Y. The geomagnetic field resembles that of a dipole whose north and south magnetic poles are located approximately (78.5° N, 69° W) and (78.5° S,111° E). The

axis being inclined 11.5° to the polar diameter and its center displaced some 300 km towards Indonesia. Since this dipole is a close approximation to the total magnetic field of the earth, its pole do not coincide with the surface points where the dip needle stands vertical i.e. where H = 0 known as the dip poles, or magnetic north and south poles, these are presently located at (75° N, 101° W) and (67° S, 143° E).Lines of equal declination D, inclination I, horizontal intensity H, etc. when plotted on maps are called isomagnetic charts. They show the variations in the geomagnetic field over the earth's surface.

(b) Origin of the main field

The main geomagnetic field theoretically could be caused by an internal or external source, either of permanent magnetism or of unidirectional current flow, or it could be the result of current flowing in and out of the earth's surface. The latter possibility can be ruled out because of the observed air-to-earth currents are much too small to account for the existing magnetic field of the earth. Spherical harmonic analysis of the observed surface magnetic fields show that at least 99% is due to sources inside, the remaining 1% to sources outside the earth.

The present theory is that the main field is caused by electric currents circulating in the outer core-known to be liquid from seismic evidence-which extends from a radius of 1300 km to 3500 km. The magnetic source is thought to be a type of self-exited dynamo, in which a highly conductive fluid moves about in complex mechanical motion, while electric currents, possibly caused by chemical or thermal variations, flow through it. The combination of motion and current creates a magnetic field. Since little is known, or is likely to be known, of the earth's core,

the theoretical development is difficult. Laboratory tests have shown, however, that the dynamo source may be a valid explanation and also that it may account for certain slow or secular variations which are known to have occurred in the earth's magnetic field.

(C) Secular variations

As a result of 400 years of continuous study, it has been established that the geomagnetic field is far from permanent. The records of I and P from magnetic observations on London and Paris extending back to about 1580, is a striking example of this. The inclination has changed some 10° (75° to 65°) and the declination about 35° (10° E to 25° W) and back to 10° W during this period. Similar wandering of the supposedly fixed field is evident from long term records of other magnetic elements. In all cases these secular variations appear to be regional rather than world wide. Although their source is not understood, it is thought to be internal, possibly connected with changes in convection currents in the core, in the core-mantle coupling and in the rotational speed of the earth.

(ii) The external field: a small fraction of the main field (about 1%) which varies rather rapidly, partly cyclically and partly randomly and which originates outside the earth, appears to be associated with electric currents in the ionized layers of the outer atmosphere. The variation in time is much more rapid than for the so-called permanent field. Several well documented effects are listed below.

(a) A cycle of 11 years duration, correlated with sun spot activity, has a latitude distribution

which indicates an external origin.

(b) Solar diurnal variations, with a period of 24 hours and range of 30γ, vary with latitude and season and are probably controlled by action of the sun on ionosphere currents.

(c) Lunar diurnal variations of 25-hour period and amplitude of about 2 vary cyclically through the month and seem to be associated with a moon-ionosphere interaction.

(d) Magnetic storms are transient disturbances with amplitudes as great as 1000γ in most latitudes and even larger in polar regions, where they are usually associated with the aurora. Although rather erratic, they often occur at intervals of about 27 days, the period correlating with sunspot activity. At the height of a magnetic storm, which may last several days, long range radio reception is considerably affected and magnetic prospecting may by impractical.

(iii) Variations of the main field (local anomalies): usually but not always much smaller than the main field, relatively constant in time and place and caused by local magnetic anomalies in the near surface crust of the earth, these are the targets in magnetic prospecting. Important changes occur in the main field as the result of variations in the magnetic mineral content of near-surface rocks. These anomalies are occasionally large enough to double the main field locally. In general they do not persist over very great distances, that is to say, magnetic maps do not exhibit large scale regional features, such as isostatic anomalies in gravity.

4.3.3 Magnetism of rocks and minerals

Magnetic anomalies are entirely caused by the amount of magnetic minerals contained in the rocks, thus it is important to deal with these minerals (which are few in number), and in particular their magnetic susceptibilities.

All material-elements, compounds, etc. can be classified in three groups according to their magnetic properties: diamagnetic, paramagnetic and ferromagnetic (the third group including several subdivisions).

(a) Diamagnetism: A diamagnetic substance is one which has a negative magnetic susceptibility. This means that in the equation $I = KH$, the intensity of magnetization induced in the substance by the field H is in the opposite direction to H. All materials are fundamentally diamagnetic, since the orbital motion of the negatively charged electrons in the substance, in the presence of the external field, H, is in such a direction as to oppose H. However, the diamagnetism will prevail only if the net atomic magnetic moment of all the atoms is zero when H is zero. This situation is characteristic of atoms with closed (completely filled) electron shells. This is a weak effect compared to other forms of magnetism. Many of the elements and compounds exhibit diamagnetism; the most common diamagnetic earth materials are graphite, gypsum, marble, quartz and salt.

(b) Paramagnetism: By definition all materials which are not diamagneitc are paramagnetic, i.e. K is positive. In a paramagnetic substance each atom or molecule has a net magnetic moment in zero external field. It is characteristic of substances whose sub-shells are not filled to the

maximum. Examples are the series of elements $_{22}$Ca-$_{28}$Ni, $_{41}$Nb-$_{45}$Rh, $_{57}$La-$_{78}$Pt,$_{90}$Th-$_{92}$U. The effect decreases with temperature.

(c) Ferromagnetism: Iron, cobalt and nickel are paramagnetic elements in which the magnetic interaction between atoms and group of atoms is so strong that there is an alignment of moments within large regions or domains of the substance. Ferromagnetism also decreases with temperature and disappears entirely at Curie temperature. Ferromagnetic minerals apparently do not exist in nature.

(d) Ferrimagnetism: materials in which the magnetic domains are subdivided into regions which may be aligned in opposition to one another, but whose net moment is not zero when H = 0 are called ferrimagnetic. Examples of ferrimagnetic minerals are magnetite, titanomagnetite and ilmenite, oxides of iron or iron and titanium, pyrrhotite

(f) Antiferromagnetism: If the nit magnetic moments of parallel and antiparallel sub-domains cancel each other in a material which would otherwise be considered ferromagnetic, the resultant susceptibility is very small, of the order of paramagnetic substances. Such a material is called antiferromagnetic for obvious reasons; hematite is the most common example.

CHAPTER 5

THE GRAVITY AND MAGNETIC DATA

5.1 INTRODUCTION

With the exception of the previous geophysical works discussed in chapter 3 that was conducted for geothermal exploration purposes, the majority of previous geophysical data were aimed at studying specific geological problems related to crustal and upper mantle structures of the Ethiopian Rift system in general (the Afar depression and the MER in particular).

Though a limited number of gravity observations were made under this survey (about 50 stations), the tasks were accomplished with data obtained from different sources and reprocessed following the procedures in gravimetry as applied to geophysics. The total number of gravity observations used are about 2220 stations. While that of magnetic data amounts about 75 stations. Both data sets were collected randomly, wherever accessibility is possible by a vehicle except to very few traverses of the gravity observations. The station separations are of semi-regional type. They generally vary from 1 to an average of about 10 km.

5.2 DATA PREPARATION AND PROCESSING

Gravity measurements have been carried out in Ethiopia since 1960. The work was not intended in establishing a standard base station network but to study geological problems related to the crustal and upper mantle phenomena of the Ethiopian Rift System. For this reason the majority of the previous data acquired are distributed in the rift system particularly the Main Ethiopian Rift, the Afar depression and the associated rift shoulders. As a consequence of this there were major problems such as lack of first and second order gravity base stations, lack of calibration lines to check the gravimeters used in the previous observations, inaccessibility of the rift shoulders, accuracy problem of altimeter height, terrain effects, absence of topographic maps at required scales such as 1:50,000, etc.

Almost the majority of the data obtained from the EIGS and AAU suffer from the effect of the above cited problems to a greater degree as compared to gravity observations made these days (e.g. the gravity observation under this survey). In addition to this the previous observations were tied to the Geophysical Observatory gravity base station whose IGSN value (g = 977452.16 mGal) was known until recently and found correctly reported in Abera's Ph.D. work (1992).

In most gravity survey reports and MSc thesis works based on these data of previous gravity surveys it is quoted that the datum value used to tie the observed values is IGSN-71 datum

when it actually is the Potsdam datum value (g = 977467.07 mGal). With the exception of to few data acquired recently and tied to the correct IGSN-71 datum value, the above misquotation of the datum value has resulted in heterogeneity in all gravity data acquired by the EIGS. Note that the difference between the IGSN-71 and the Potsdam reference gravity values of the main gravity base station at the Geophysical Observatory is 14.91 mGal. The consequence of this heterogeneity has generated quite a considerable trouble in homogenising the data used in this study. To alleviate this problem of datum inhomogenity corrections were made to the previous data obtained from the sources mentioned below.

Sources of gravity data

The data that are used in this thesis work are obtained from

- field work collected by the author of this thesis and Dr. Abera in February 1999, (about 50) stations
- Geophysical Observatory (Abera's Ph.D. work), and
- the Ethiopian Institute of Geological Surveys (EIGS)

The instrument used to collect the gravity data (about 50 stations) was a La-Cost and Romberg gravimeter (model G-781), obtained from Geophysical Observatory of AAU.

A total number of about 2220 gravity stations were used to work on the gravity prospecting method. Data were checked whether they are connected to the IGSN-71 datum or to the Potsdam datum with:

- reobservations made on previously observed identical stations in the study area and

- computations made on theoretical considerations using a FORTRAN program developed by Dr. Abera. This program computes gravity anomalies using observed relative gravity values referred to the two datum (IGSN and Postsdam) with theoretical gravity (γ) values calculated according to GRS-1930 and GRS-1967 and finally determines which particular observed gravity value is connected to which particular datum.

The measures taken above resulted in heterogeneity of datum for almost all the previous data obtained and proved that the observed gravity values obtained from both sites were not available to the IGSN-71 datum; even if they were reported to this datum. Hence, reprocessing and re-evaluation of the previous data became an inevitable task in order to keep the consistency between the data sets.

Accordingly, all the previous data were reprocessed with ties made to the IGSN-71 station of the Geophysical Observatory. Theoretical gravity computed according to GRS-67 formula and the standard corrections discussed in chapter 4 were properly applied with a uniform density of 2.67 gm/cm^3, to compute the Free-air and the Bouguer anomalies. Furthermore, the level of error of the computed point Bouguer anomalies at each station is determined according to the scheme outlined in section 5.3 here below and is estimated at ± 2.82 mGal. The reduction process was performed using a FORTRAN program developed by Dr. Abera (1999).

Terrain corrections were made for about 434 stations obtained from EIGS, AAU and the 50 stations observed under this survey. An estimated error of about 2 mGal was considered due to neglect of terrain effect for the rest of the stations. This estimate was based on a statistical value calculated along two traverses that cross the Aluto mountain (2335 m), rising about 700 m above the rift floor by Dr. Abera (1992). This value is thought to apply for all stations and treated as systematic error in computing the over all mean square error of the computed point gravity anomalies.

All the gravity stations occupied have been referred to the IGSN-71 datum (Morelli etal.,1971). The primary base station used was that of the Geophysical Observatory IGSN-71 base station (977452.16 mGal) located at Addis Ababa University. The magnetic observations were corrected for diurnal variation with reference to the respective base stations of each traverse considered. The base stations considered were occupied / read at the beginning and end of each observation session of the traverses to reduce and eliminate any diurnal variations that may appear during the day's work.

Sources of magnetic data

The magnetic data were collected using a proton precision magnetometer (from the Department of Geology and Geophysics) that measures the total intensity of the earth's geomagnetic field. About 75 different magnetic stations were covered by the author of this paper and Dr. Abera Alemu.

5.3 ASSESSMENT OF ERRORS IN THE GRAVITY ANOMALIES

The assessment, computation and evaluation of the errors involved in the computed point Bouguer anomalies are reported by Abera (1992, 1998) as adapted here below.

In analysing the accuracy of computed point gravity anomalies it is necessary to appraise the accuracy of the method used in computing them, i.e., the completeness of the formula used and the correctness of the numerical values of the constants occurring in it (Abera, 1992). A systematic error may be introduced in the computed Bouguer anomalies, for example by neglecting the correction for irregularities in the topography (terrain correction).

It is also necessary to assess the effect of random and systematic errors of the parameters of the formula, the values of which are determined separately for each gravity point.

These include the errors involved in the determination of:

★ the observed value of gravity (observation error or measurement precision) at each station

★ the point elevations (elevation error) at each station

★ the geodetic latitude (latitude error)

★ the reduction density (density error) of the topographic masses above sea level used in the computation of the Bouguer anomaly values at each station.

We know that the computation of the point Bouguer anomalies values, Δg_B, for each observation point is performed with the formula:

$$\Delta g_B = g + 0.3086h - 0.04191\rho h + \delta g_t - \gamma \qquad (5.1)$$

The accuracy, $\sigma_{\Delta g}$, in the determination of the point Bouguer anomalies, Δg_B, is dependent on the precision in the determination (observation error) of the parameters g, h, ρ and ϕ, involved in the formula.

Since the values of g, h, ρ and ϕ are determined separately for each gravity point, the precessions (observation errors) σ_g, σ_h, σ_φ and σ_ρ in the determination of g, h, ρ and ϕ respectively are independent to each other (i.e., are uncorrelated).

The overall mean square error $\sigma_{\Delta g}$ of the gravity anomalies, is

defined by

$$\sigma^2_{\Delta g} = \delta^2_{\Delta g} + s^2_{\Delta g} \qquad (5.2)$$

where $\delta_{\Delta g}$ is the standard error (due to random errors) and $s_{\Delta g}$ is the systematic error (bias) of the gravity anomalies, Δg_B.

The variance $\delta^2_{\Delta g}$, can be computed from the law of propagation of errors for uncorrelated observations according to the following scheme:

Since the Bouguer anomaly formula is a function of the parameters g,h,ρ and ϕ, it's implicit functional form is given by

$$\Delta g = \Delta g(g,h,\rho,\phi) \qquad (5.3)$$

The differential of Δg is expressed as

$$d\Delta g = (\partial\Delta g/\partial g)\,dg + (\partial\Delta g/\partial h)\,dh + (\partial\Delta g/\partial\rho)\,d\rho + (\partial\Delta g/\partial\phi)\,d\phi = \delta_{\Delta g} \qquad (5.4)$$

The partial derivatives on the right hand side of Eq. (5.4) above are independently evaluated upon substitution of Δg by the Bouguer anomaly formula, $\Delta g_B = g_{obs} + 0.3086h - 0.04191\rho h - \gamma$.

The individual contributions to the standard error, $\delta_{\Delta g}$, due to the random errors (unavoidable errors) that occur naturally in the process of measuring (observing, determining) the relative point gravity values, point elevations, point geodetic latitudes of the gravity stations and density of the topographic masses are modelled and evaluated as follows.

★ The first partial derivative of Eq. (5.3) results in

$$(\partial \Delta g/\partial g)\, dg = (dg/dg)\, dg = dg = \sigma_g \qquad (5.5)$$

and corresponds to the measurement precision (observation error) of the observed relative gravity values evaluated as follows.

Actual field tests made with observations taken at 4 national base stations (check points) located in Addis and its environs (Table 1), consists a summary of 12 independent observations made at 4 gravity check-points (national base stations), that means, 3 independent observations at each check point.

The measurement precision, σ_g, is obtained by computing the internal variance (Bjerhammer, 1973) of the 12 independent observations made at the 4 gravity check points following the

scheme outlined in Table 1 and the formula:

$$\sigma^2_g = (\Sigma_{s1}(vv) + \Sigma_{s2}(vv) + \Sigma_{s3}(vv) + \Sigma_{s4}(vv))/(n-s) \quad (5.6)$$

where n is the total number of independent observations, s_1, s_2, s_3 and s_4 are the number of gravity check points, and v are residuals for the individual observations at each check point.

Table 1. Table of observed relative gravity values (mGal) for computing the internal variance of 12 independent observations taken at 4 check points.

	y	$\hat{y}$	v	vv	
S1:	1015.90	1015.92	-0.02	0.0004	$\Sigma_{s1}(vv) = 0.0078$
	1015.99	1015.92	0.07	0.0049	
	1015.87	1015.92	-0.05	0.0025	$\hat{y}_1 = 1015.92$
S2:	0994.99	0994.92	0.07	0.0049	$\Sigma_{s2}(vv) = 0.0083$
	0994.89	0994.92	-0.03	0.0009	
	0994.87	0994.92	-0.05	0.0025	$\hat{y}_2 = 0994.92$
S3:	1030.67	1030.69	-0.02	0.0004	$\Sigma_{s3}(vv) = 0.0078$
	1030.76	1030.69	0.07	0.0049	
	1030.64	1030.69	-0.05	0.0025	$\hat{y}_3 = 1030.69$
S4:	1027.71	1027.74	-0.03	0.0009	$\Sigma_{s4}(vv) = 0.0083$
	1027.81	1027.74	0.07	0.0049	
	1027.69	1027.74	-0.05	0.0025	$\hat{y}_4 = 1027.74$

Findings of this investigation indicate that the gravimeter has a measurement precision computed using Eq. (5.6) as,

$$\sigma_g = \pm [(0.0078 + 0.0083 + 0.0078 + 0.0083)/(12-4)]^{\frac{1}{2}}$$

$$= \pm 0.06 \text{ mGal}$$

$\sigma_g = \pm 0.06$ mGal is therefore, the computed observation error estimate (the overall reproducibility of the gravimeter) that one may encounter when taking readings with this gravimeter.

★ The second Partial derivative of Eq. (5.3) results in,

$$(\partial\Delta g/\partial h)dh = d/dh(0.3086h-0.04191\rho h)dh \qquad (5.7)$$

➢ By making use of the adopted reduction density, $\rho = 2.67$ g/cm^3 and the precision in the elevation determination, $\sigma_h = 10$ m, reported , the error introduced in the computed Bouguer anomalies due to elevation error is computed to amount to:

$$(0.3086-0.04191 \times 2.67)\sigma_h = \pm 1.97 \text{ mGal.} \qquad (5.8)$$

★ The third partial derivative of Eq. (5.3) results in,

$$(\partial\Delta g/\partial\rho)d\rho = d/d\rho(0.04191\rho h)d\rho \qquad (5.9)$$

➢ Supposing that we want to achieve a reduction precision of

0.2 mGal in the Bouguer reduction using the Bouguer plate gravity formula given by

$$g_{BP} = 2\pi G\rho h = 0.04191\rho h \qquad (5.10)$$

The precision of density determination, which is required for the computation of Bouguer anomalies follows as,

$$\sigma_\rho = d\rho = (1/0.04191h)dg_{BP} \qquad (5.11)$$

For the mean elevation, h = 1869.15 meters, of the gravity stations we considered within the limits of the study area in the application of the reduction density, ρ = 2.67 g/cm^3, the precision of adopting this density value would amount to,

$$\sigma_\rho = (1/0.04191 \text{ x}1869.15) \text{ x } 0.2 = 0.0026 \text{ g/cm}^3 \qquad (5.12)$$

The error introduced in the computation of the point Bouguer anomalies due to density error is therefore computed as,

$$(\partial\Delta g/\partial\rho)d\rho = (0.04191 \times h)\sigma_\rho = \pm 0.20 \text{ mGal} \qquad (5.13)$$

★ The last partial derivative of Eq. (5.3) results in,

$$(\partial\Delta g/\partial\phi)\, d\phi = 1/R\,(\partial\gamma/\partial\phi)\, d\phi \qquad (5.14)$$

➢ By differentiating the expression for the normal gravity given by Eq.(4.20), with respect to ϕ and letting R = 6371229m (mean earth's radius), the rate of change of the normal gravity with latitude is estimated by

$$1/R\,(\partial\gamma/\partial\phi) = 0.813 \sin 2\phi \text{ mGal/km} \qquad (5.15)$$

For the mean latitude, $\phi \leq 7.25°$ of the study area, the variation in the normal gravity is about 0.000203 mGal for each meter travelled in a N-S direction. Thus, for each meter error north or south in the measured position of an observation site, an error of 0.000203 mGal (0.000203mGal/m) will be introduced in the value of γ.

For the precision estimate, $R\sigma_\phi = \pm$ 200 m, in the determination of the latitude (UTM co-ordinates) of the gravity stations scaled from 1:250,000 and 1:50,000 topo maps, the error estimate in the normal gravity reduction for the computation of the Bouguer anomalies amounts to:

$$1/R\,(\partial\gamma/\partial\phi)\, R\sigma_\phi = 0.04 \text{ mGal (for } \phi \leq 7.25°) \qquad (5.16)$$

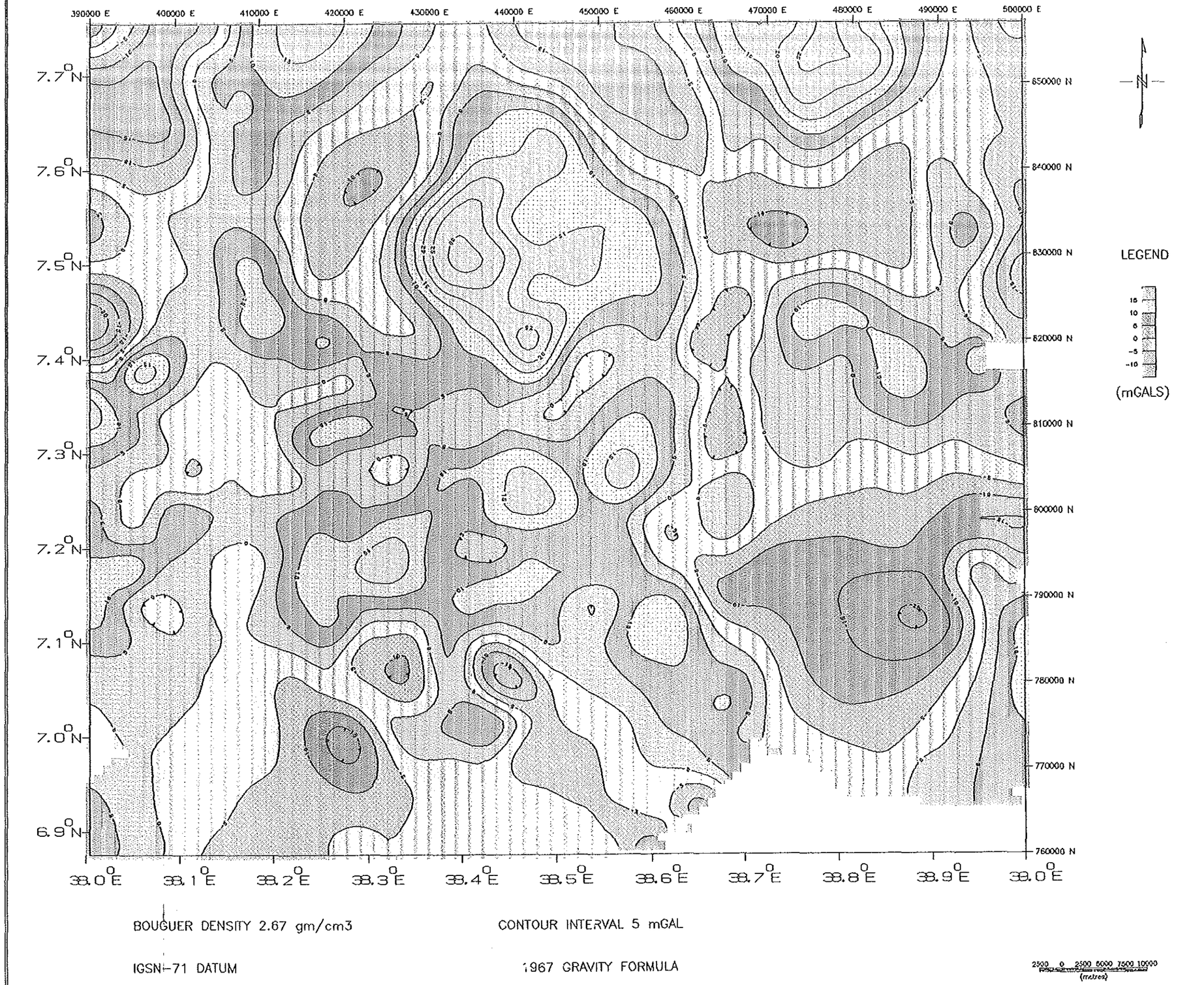

Fig.5 RESIDUAL ANOMALY MAP OF CORBETTI AND ITS SURROUNDING AREA.

5.4 COMPILATION OF THE GRAVITY ANOMALY MAPS

As a rule of thumb, the first step in the interpretation of a geophysical survey data is compilation of anomaly map of the area.

The computed Bouguer anomaly values and the total magnetic field values are reported as Free - air anomaly map (Fig.4), Bouguer anomaly map (Fig.3) and total magnetic field map (Fig.8) by plotting them on 1:250,000 scale map of the study area. The contouring is made in 5 mGal and 100 gamma contour interval (CI) isoanomaly curves. The task is performed using the standard gravity and magnetic mapping software, Geosoft (1996).

With very few exceptions, the stations exhibit consistent trends of the gravity values, thus demonstrating the overall good quality of the survey.

The judgement made on the quality of the survey and the choice of the contour interval (CI = 5 mGal) employed in the compiled Bouguer anomaly map are based on the level of error of the point Bouguer anomalies determined in section 5.3 and estimated at ± 2.82 mGal.

Furthermore, the separation of the regional effect from the Bouguer anomaly was performed using a computer program based on the trend surface of the regional gravity anomaly approximated using a polynomial surface fitting of degree 3. The corresponding residual anomalies were then obtained, and using the same square grid interpolation, the regional anomaly

map (Fig.6) and residual anomaly map (Fig.5) are produced. Preliminary qualitative interpretation of these maps has been made using as a constraint, the geological and / or structural map (Fig.2) of the MER, compiled by G.M. DI Paola (1972), and the results of previous geophysical surveys discussed in chapter three.

5.5 INTERPRETATION OF GRAVITY DATA

5.5.1 Bouguer anomaly map:

The Bouguer gravity anomaly map (Fig. 3) is prepared with a contour interval of 5 mGal. It shows anomaly features ranging from a minimum value of -255 mGal to -190 mGal, which is a typical characteristic feature of the rift system. This map reveals an overview of the topographic feature and underlying crustal structures. The distinction between the rift and the adjacent plateaux and the regional structure features were depicted from the map on the basis of the general shape and wavelengths of the anomalies. However, anomalies on the Bouguer map have no great significance on the structural and geological features of shallow origin. Separation of the regional and residual gravity anomalies from the Bouguer gravity map and their qualitative interpretation led to defining the anomalies related to deep structures, and local anomalies of shallow origin respectively.

As shown in the previous works of Mohr and Gouin (1967,68) the rift valley is in gravity "low". The broad negative anomaly of the rift shown on the Bouguer map trends approximately N-S between longitudes 38.50^{0}E and 39.00°E and curves to NNW-SSE orientation towards the

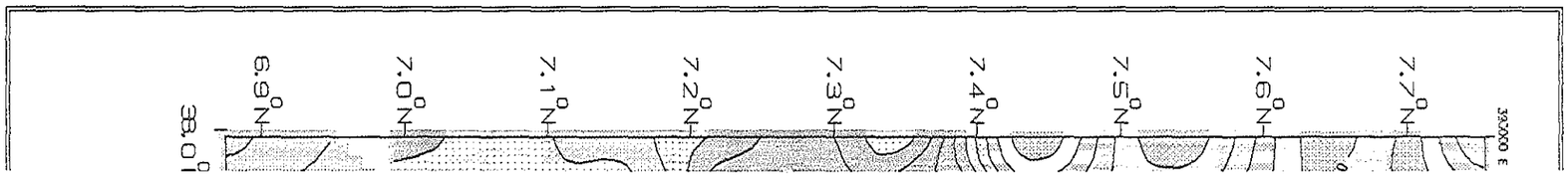
6.9°N
7.0°N
7.1°N
7.2°N
7.3°N
7.4°N
7.5°N
7.6°N
7.7°N
38.0°
E

A large two dimensional gravity high is oriented in a NW-SE direction (shown as P_3 and P_4) which includes the Corbetti caldera. This anomalous zone is characterised by intensive surface fumarolic activity. It can be associated with high density materials of the subsurface materials. In the north central portion part of the map relative positive anomalies are present at the volcano-tectonic Shalla caldera which is in filled by lake Shalla water. This relative positive anomaly P_2 is located at the co-ordinates of about (38.4°E,7.5°N) which is the locality of lake Shalla, implying that higher density subsurface material are dominant and associated in the Shalla caldera.

The general view of the Bouguer anomaly map resembles that of the topographic (elevation) map (Fig. 9) in that, the eastern escarpment of the rift is represented and shown clearly by a N-S alignment of the contours marking the boundary between the relative positive and relative negative responses. The elevated high lands are delineated by these relative negative high responses.

5.5.2 The free air anomaly map:

Responses of the free air anomaly range from a minimum value of about - 65 mGal to about more than 80 mGal (Fig. 4). This map is produced with a contour interval of 5 mGal.

There is a close correlation between the pattern of the free air anomaly and the topography of the study region, which are observable on figures (4) and (9). This map is limited to support in the

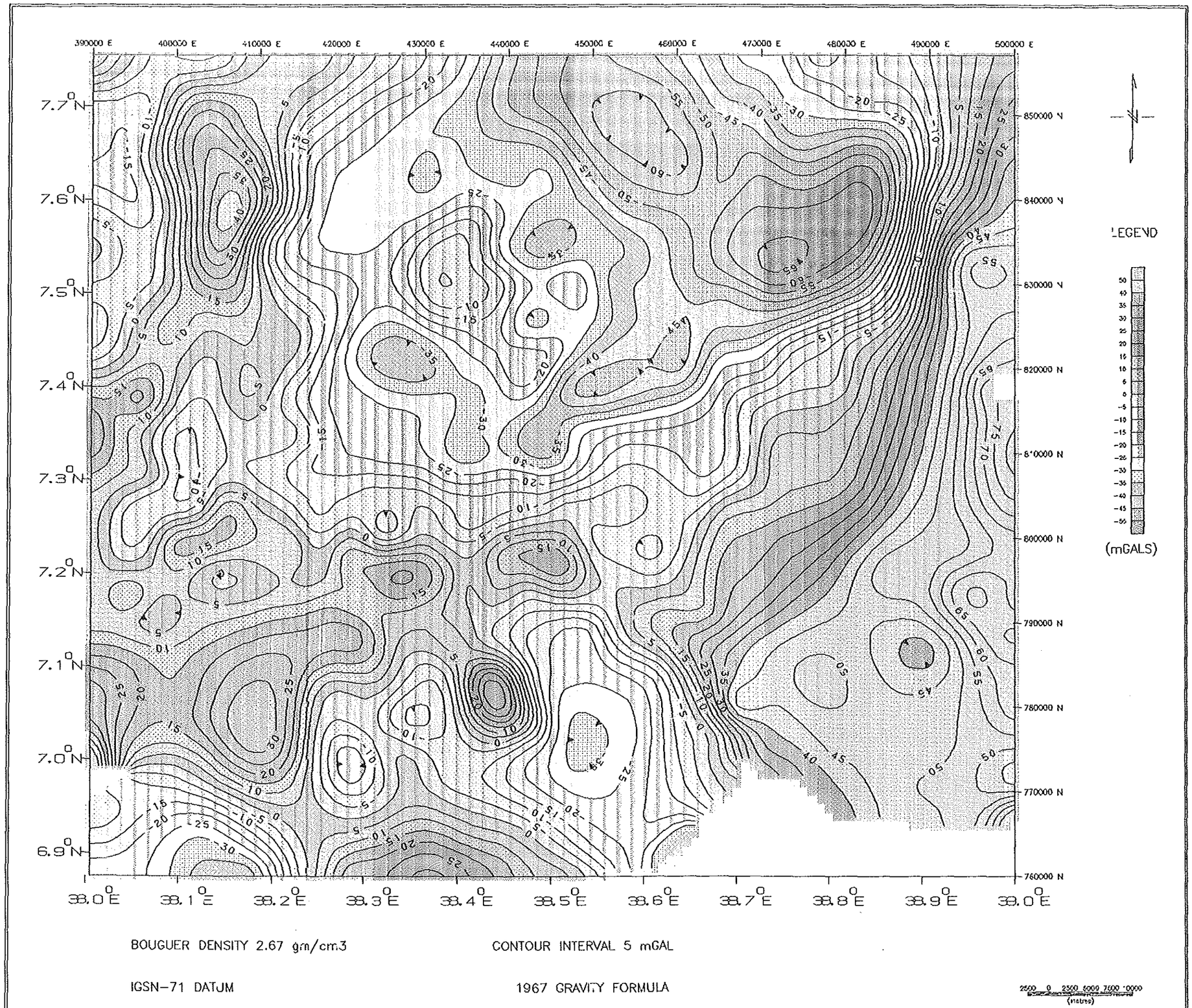

Fig.4 FREE AIR ANOMALY MAP OF CORBETT AND ITS SURROUNDING AREA.

interpretation of the Bouguer anomalies, since an over all correlation can not be obtained between the anomalies and the subsurface geological features. However, the N-S running rift shoulder that was revealed by the Bouguer map is also indicated on the free air map (at the eastern part). The high lands are indicated by positive free air values.

Negative values are more dominant in the central northern part of the area , while Corbetti area is characterised mostly with moderate positive responses.

5.5.3 The residual anomaly map:

The residual anomaly is prepared with a contour interval of 5 mGal (Fig. 5). The residual is part of the picture left after subtraction of the regional gravity field. Thus, the choice of the regional dictates the nature of the residual map. Residual gravity is a term arising out of the fact that the conventional gravity map reflects the superposition of local gravity fields (anomalies) due to local geological structures, upon those of gravity fields caused by regional geological structures.

Local positive and negative anomalies are shown on the residual anomaly map with amplitudes varying from -20 to +30 mGals. The broadest positive anomaly is shown as two dimensional striking NW-SE and includes the Urji volcano, which is in agreement with the Bouguer response as explained above. It is associated with fumarolic activities beginning from the Corbetti caldera and extending NW wards. Chabbi has an offset positive anomaly within the caldera. The largest positive anomaly is centred on a recent basalt flow south of lake Shalla and a less positive anomaly is observable at lake Shalla which has hot springs at the southern shore.

5.5.4 The regional anomaly map:

The regional anomaly map which was extracted from the Bouguer map shows smoothed large scale regional features. The regional anomaly map (Fig. 6), shows gravity features whose values range from -244 to -196. The map indicates that these values increase from east towards the west. The low regional gravity gradient on the Ethiopian plateau also increases north eastward, which according to Mohr and Rogers (1966), is not evidenced in the thickness of the trap series or the Mesozoic sediments, nor the geology of the basement, but must be related to the thinning of the crust. The wide negative regional anomaly on the Ethiopian plateau could possibly be associated to the thickness of the crust beneath the surface.

5.5 Interpretation of magnetic data

The field magnetic data were very limited, i.e. the aerial coverage is confined to only Corbetti areas. Thus, the map is used in the combined interpretation of the various gravity maps. As stated earlier the total number of stations are about 75. Figure (8) shows the magnetic anomaly map of Corbette and its surroundings. From this map we observe that values of the total field magnetic data range from about 34600 - 35300 gamma. From the trends of the magnetic contours one can observe a NW-SE alignment. This feature is observable on the Bouger map and is qualitatively interpreted as a two dimensional relative positive anomaly (marked as P_3 to P_4 Fig. 3). The Corbetti caldera is characterised by lower magnetic responses which is in the average value of about 34900 gamma.

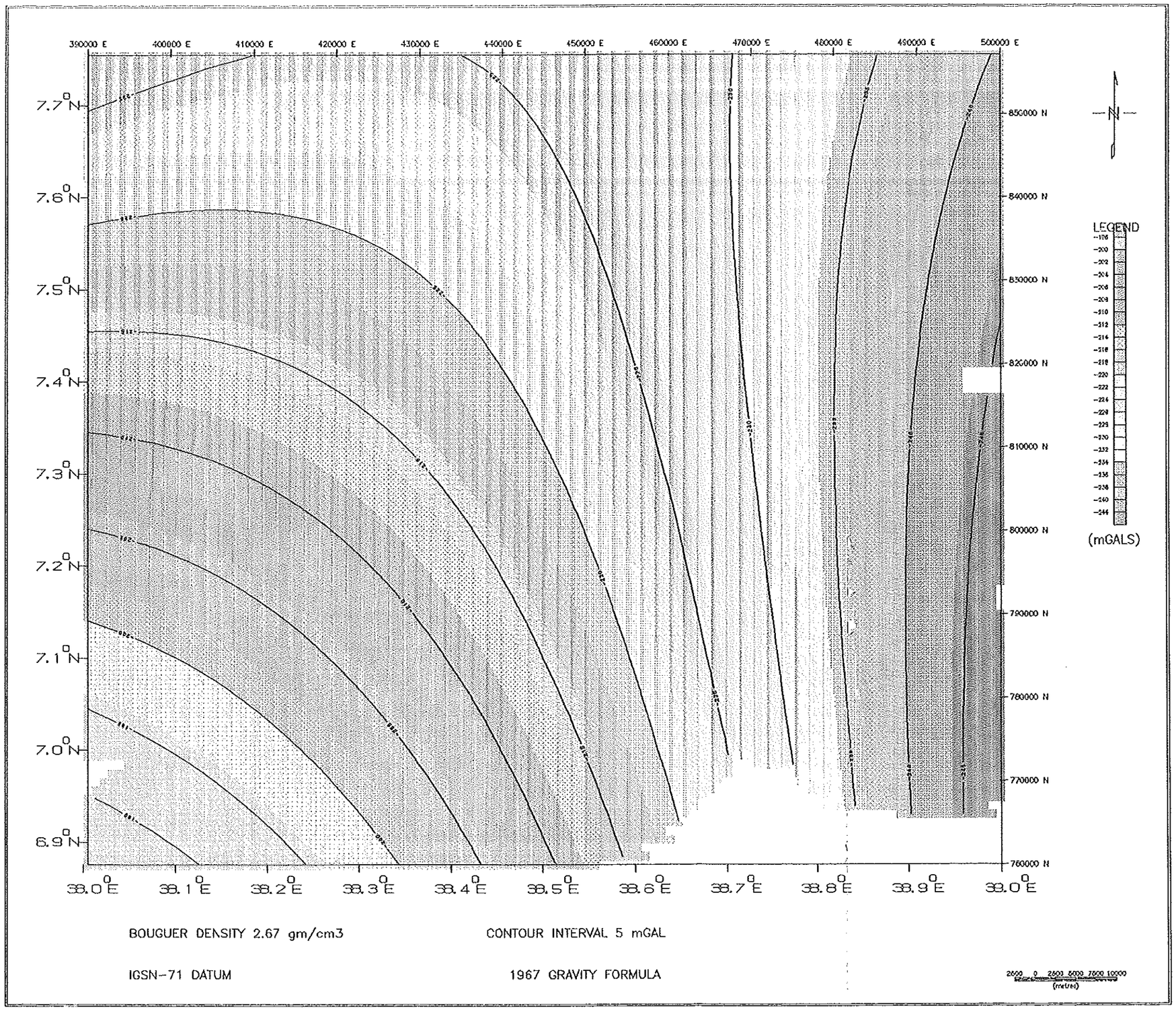

Fig.6 REGIONAL ANOMALY MAP OF CORBETTI AND ITS SURROUNDING AREA.

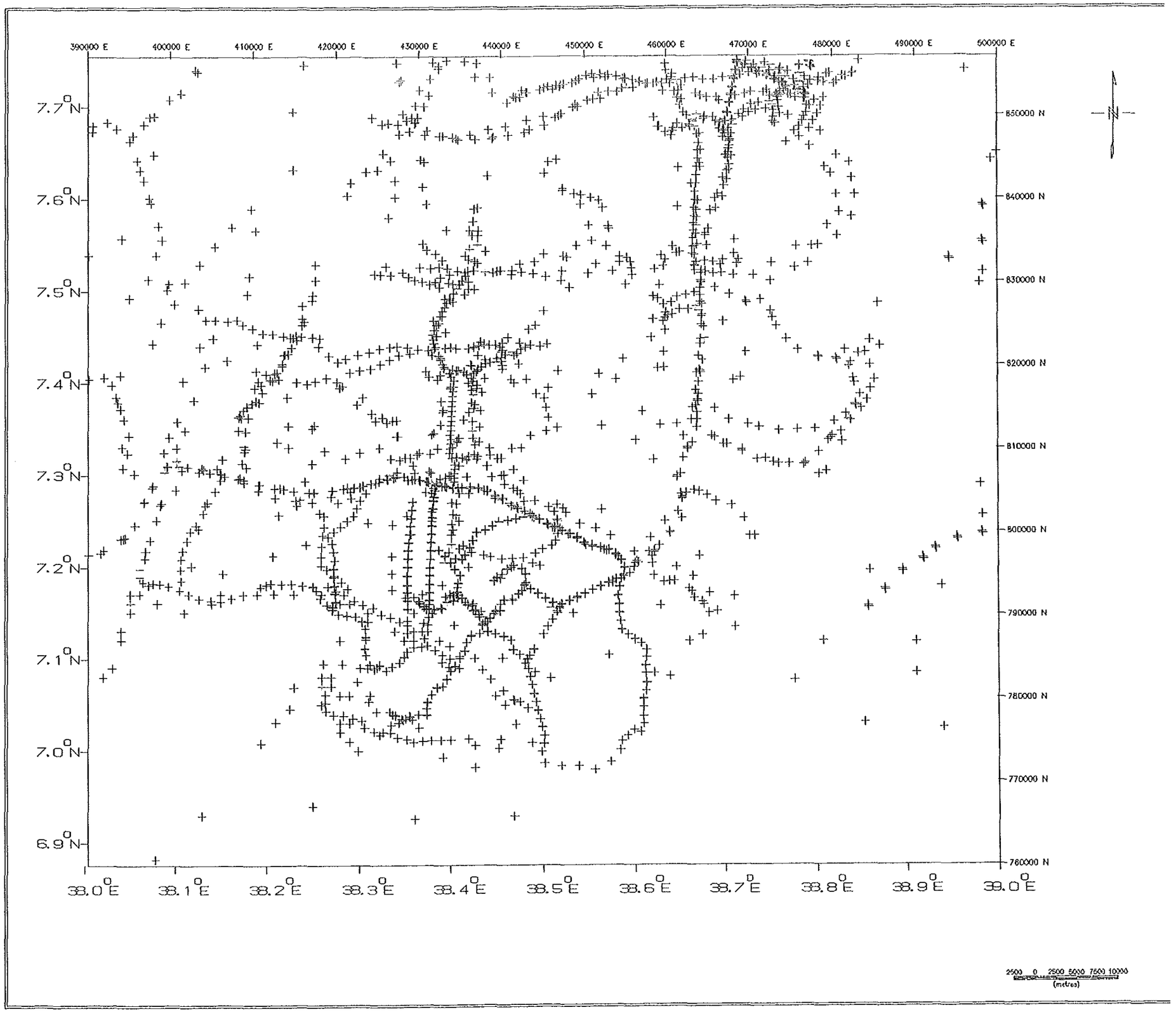

Fig.( ) GRAVITY STATIONS (+) MAP OF CORBETTI AND ITS SURROUNDING AREA.

From the alignment of the contours of the magnetic data and the gravity anomalies we observe that they are in agreement by mapping similar trends of geologic bodies.

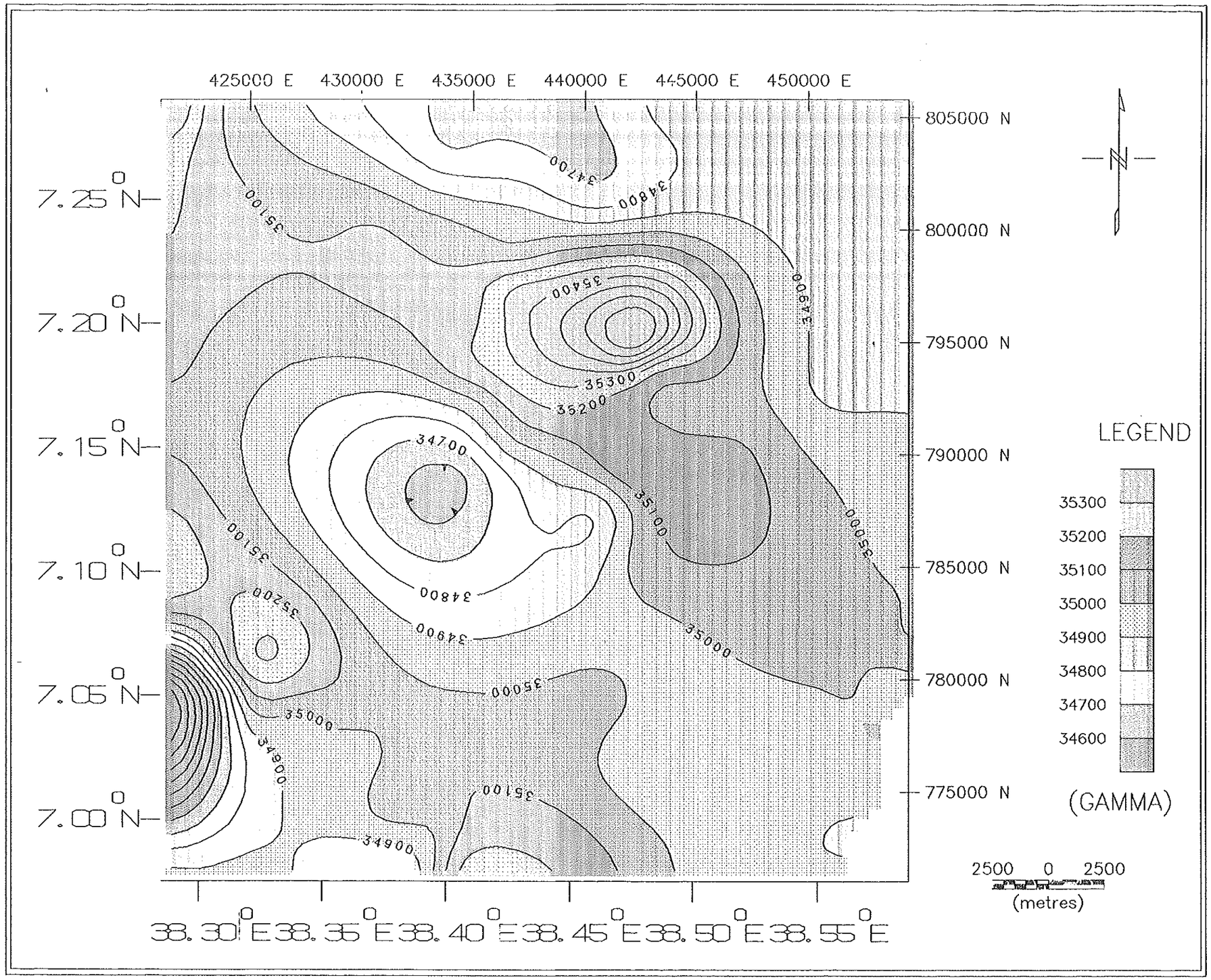

Fig.( ) MAGNETIC (TOTAL FIELD) MAP OF CORBETTI AND ITS ADJACENT AREA.

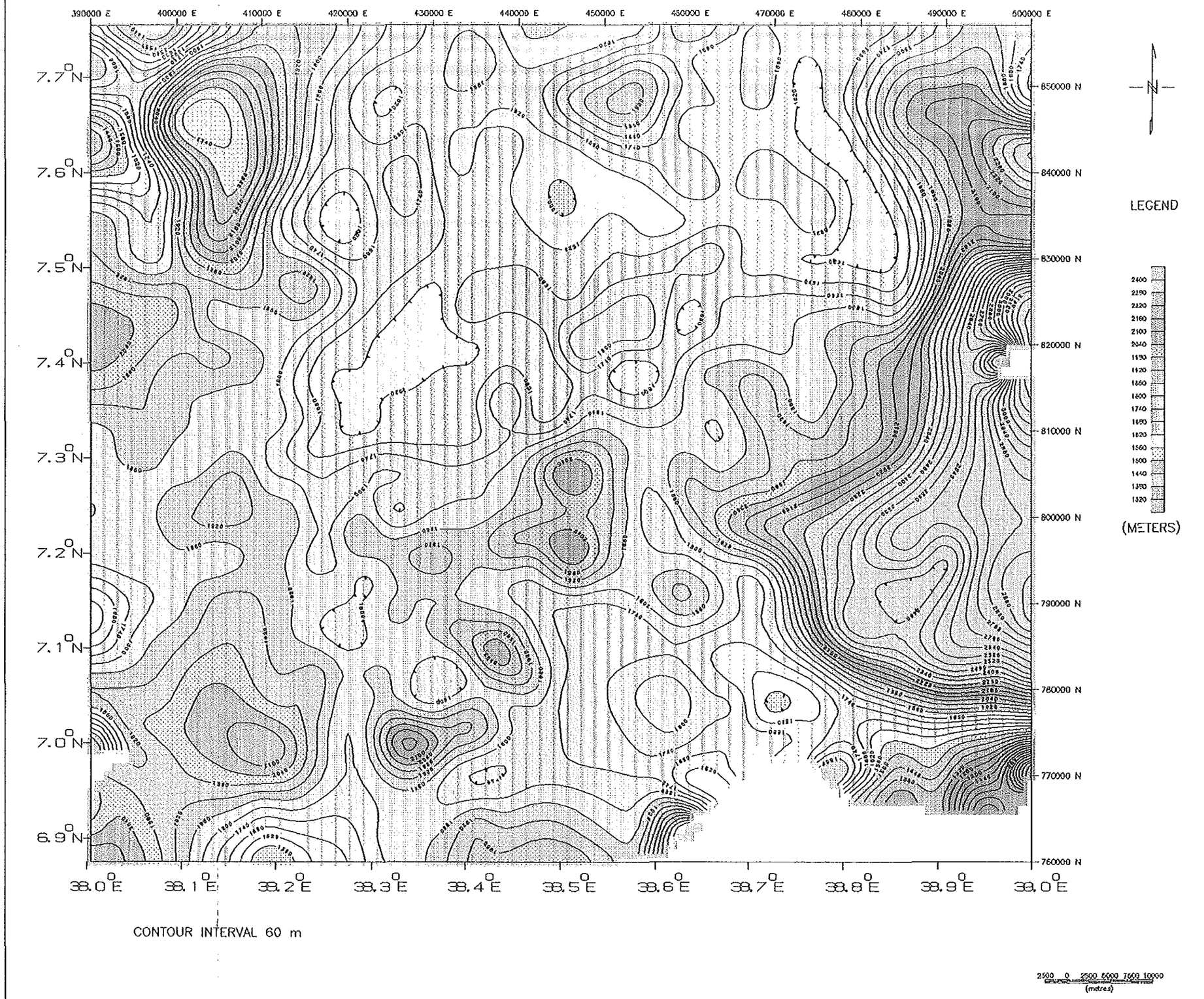

Fig.9 ELEVATION MAP OF CORBETTI AND ITS SURROUNDING AREA.

CHAPTER 6

CONCLUSIONS AND RECOMMENDATIONS

6.1 DISCUSSION

Makris et.al (1969, 1970) have published papers on crustal and upper mantle models from gravity measurements across the northern sector of the MER and the Afar Depression. These models show a thinning of the crust layers from south to north and an intrusion of upper mantle material beneath the rift. There is a fair agreement with the concept that, north to south, in Ethiopia, we proceed from the oceanic crust of the central Red Sea Graben to the major crustal thinning with some oceanic crust at Earte Ale in Afar (Makris, 1972) and to the Wonji Fault Belt (WFB) - the axis of the Main Ethiopian Rift.

From the forgoing analysis of the gravity and magnetic data, the prominent point that can be highlighted is the correlation between gravity and magnetic trends and structures of the rift system including the study area, Corbetti, (gravity and magnetic anomaly maps). It has been observed that the axes of positive anomalies, are associated with rift floor and belts of synclinal structures. The negative axes, on the other hand are associated with the uplifted regions and belts of anticlinal structures.

6.2 CONCLUSIONS AND RECOMMENDATIONS

Both the gravity and magnetic data over Corbetti and its adjacent areas have revealed and confirm the structural weak zones which are characterized by faults, fractures and the like. The standardization of the available gravity data have also been done so that other workers in the area can have make use of it.

The main conclusions of this study are:

There is an inverse correlation between the topographic relief and the gravity field in the study region. This is associated with isostatic compensation of the topographic relief by low density material at depth (Makris et. al., 1975). This is proved to be acceptable. A qualitative interpretation of the complied Bouguer map, using the existing limited geological and structural information, has revealed the inverse correlation between the topographic relief and the Bouguer anomalies. The Bouger anomaly map (Fig. 3) clearly shows that the elevated areas are characterised by gravity minima -255 mGal. While the lower altitudes are characterised by relative positive anomalies.

Local maxima and minima superimposed on the broad negative regional anomaly show the existence of structural units having density contrasts with the surroundings. The gravity anomaly map shows maxima and minima that are separated by contour lines of equal gravity value. The maxima correspond to the central parts of rock masses that have a density which contrasts with

that of the surroundings.

The qualitative interpretation of the gravimetric maps is to identify and locate geological units their boundaries and structure indications. The existing geological features and some isolated structural units identified in the previous works are further confirmed. With regard to this the Bouguer map, the free air map and the residual map, have revealed several structures such as the eastern rift shoulder and other minor en echelon type faults.

Besides mapping the structural indications present in the study area, these maps have delineated areas with higher subsurface denser materials, as shown by relative positive anomalies that are supposed to be caused by the intrusion of mantle materials. The relatively positive anomaly of the MER is associated by the mass deficiency providing isostatic balance of the regional uplift to compensate for the relatively lower elevation of the rift floor as it was concluded by Gouin (1972).

As it has been stated in the objective of this thesis work, the available gravity data with in the study region were reduced to the IGSN-71 datum, which is considered to be in a standard format. The availability of these data will provide researchers with a considerable information of the gravity field of the study region and could be applied for further research program intended to be conducted in the area.

Recommendations:

In view of the above conclusions, it is therefore essential to complement and refine the study of this survey by additional geophysical work such as refraction seismic, wider area coverage of magnetic survey, transient electromagnetic (TEM) sounding, etc. By doing so, without doubt further refinement of the observations, and consequently of better interpretations of the area can be arrived at. Besides these the data can also be used for other purposes, such as exploration of potential economic resources like geothermal energy resources, sulfide minerals, epitermal gold deposits etc.

REFERENCES

Abera, A., 1983. Crustal Modelling from Gravity Data in the Ethiopian Rift. Ms. Thesis, Addis Ababa University, Addis Ababa, Ethiopia.

Abera, A. 1988. Gravity Field Interpretation Over the Main Ethiopian Rift. Proceedings of the 6th International Symposium "Geodesy and Physics of the Earth", Potsdam, Part II, pp. 99-115.

Abera, A. 1999. A FORTRAN program to compute Bouguer and free-air anomalies with a choice of appropriate reduction density (unpublished report)

Abera, A., Sj`berg, L.E., 1990. Gravity Field Interpretation and Crustal Model Studies in the Main Ethiopian Rift. Presented at the Third International Symposium on Recent Crustal Movements in Africa. 8-16 December 1990, Aswan, Egypt.

Abera, A., 1992. The Gravity Field and Crustal Structure of the Main Ethiopian Rift. Ph.D. Thesis, Royal Institute of Technology, Department of Geodesy, Report No. 26 (TRITA GEOD 1026), Stockholm, Sweden.

Abera, A., 1998. The Gravity Survey of the Tana-Beles Hydroproject Tunnel Site. A Geotechnical report submitted to the Aquatech Pvt. Ltd. Company, Addis Ababa, Ethiopia (unpublished).

Abera, A., 1999. An interactive FORTRAN program that checks the datum that an observed relative gravity is tied to and computes and computes the point Free-air and Bouguer anomaly values of a station

Baker, B.H. Mitchell, J.G., 1976. Volcanic Stratigraphy and Geochronology and the Kedong-Olorgesaile Area and the Evolution of the South Kenya Rift Valley. J.Geol. London 132: 467-484.

Baker, B.H., Mohr, P.A. and Williams, L.A.J., 1971. Geology of the Eastern Rift System of Africa. Geol. Soc. Amer. Spec. Pap., pp 136-167.

Baker, B.H., Mohr, P.A. and Williams, L.A.J., 1972. Geology of the Eastern Rift System of Africa Geol. Soc. Amer. Spec. Pap., pp 136-67.

Baker, B.H., and Wohlenberg, J., 1971. Structured and Evolution of the Kenya Rift Valley. Nature, 229: 538-542

Di Paola, G.M., 1972. The Ethiopian Rift Valley (between 7(and 8(40Æ Lat. North) Bull. Volc. 36: 517-560.

Grant, F.S and West, G.F., 1965. Interpretation Theory in Applied Geophysics.

Gibson, I.L, 1969. The Structure and Volcanic Geology of an Axial Portion of the Main Ethiopian Rift, Tectonophysics, Vol. 8, pp 561-565

Oluma, B., 1989. The application of gravity and electrical resistivity surveys to geothermal exploration in the Main Ethiopian Rift. M.Sc. Thesis. University of Leicester, England.

Oluma, B., et. al.,1983. Corbetti Geophysical Exploration I

Parasnis, D.S., 1968. Principles of Applied Geophysics, fourth edition, Chapman and Hall, U.S.A.

Searl, R.C., and Gouin, P., 1972. A Gravity Survey of the Central part of Ethiopian Rift

Valley. Tectonophysics, Vol. 15, pp 41-51.

Telford, W.M., Sheriff, R. E., and Geldart, L. P., 1990. Applied Geophysics, second ed.

Cambridge, Cambridge University Press.

Tsuboi, C., 1983. Gravity. George Allen and Unwin publishers Ltd. U.K. 5.3